

JGR Biogeosciences



RESEARCH ARTICLE

10.1029/2022JG007072

Key Points:

- The heterogeneity in Arctic drainage basins creates a north-south separation in Mn contributions to the Canadian Arctic Archipelago ocean
- Glacial runoff from Nares Strait supplies micronutrients such as Mn to the Pikiyasorsuaq or North Water polynya
- Changes in glacial runoff composition in the Canadian Arctic Archipelago and northwestern Greenland are conveyed downstream into Baffin Bay

Supporting Information:

Supporting Information may be found in the online version of this article.

Correspondence to:

B. Rogalla,
brogalla@eoas.ubc.ca

Citation:

Rogalla, B., Allen, S. E., Colombo, M., Myers, P. G., & Orians, K. J. (2023). Continental and glacial runoff fingerprints in the Canadian Arctic Archipelago, the Inuit Nunangat Ocean. *Journal of Geophysical Research: Biogeosciences*, 128, e2022JG007072. <https://doi.org/10.1029/2022JG007072>

Received 30 JUN 2022
Accepted 18 APR 2023






Author Contributions:

Conceptualization: B. Rogalla, S. E. Allen, M. Colombo
Formal analysis: B. Rogalla
Funding acquisition: S. E. Allen, P. G. Myers, K. J. Orians
Investigation: B. Rogalla, M. Colombo
Methodology: B. Rogalla, S. E. Allen, M. Colombo
Software: P. G. Myers
Supervision: S. E. Allen, P. G. Myers, K. J. Orians
Visualization: B. Rogalla
Writing – original draft: B. Rogalla

© 2023 The Authors.

This is an open access article under the terms of the [Creative Commons Attribution-NonCommercial License](https://creativecommons.org/licenses/by/4.0/), which permits use, distribution and reproduction in any medium, provided the original work is properly cited and is not used for commercial purposes.

Continental and Glacial Runoff Fingerprints in the Canadian Arctic Archipelago, the Inuit Nunangat Ocean

B. Rogalla¹ , S. E. Allen¹ , M. Colombo² , P. G. Myers³ , and K. J. Orians¹ 

¹Department of Earth, Ocean, and Atmospheric Sciences, University of British Columbia, Vancouver, BC, Canada,

²Department of Marine Chemistry and Geochemistry, Woods Hole Oceanographic Institution, Woods Hole, MA, USA,

³Department of Earth and Atmospheric Sciences, University of Alberta, Edmonton, AB, Canada

Abstract Rising temperatures and an acceleration of the hydrological cycle due to climate change are increasing river discharge, causing permafrost thaw, glacial melt, and a shift to a groundwater-dominated system in the Arctic. These changes are funneled to coastal regions of the Arctic Ocean where the implications for the distributions of nutrients and biogeochemical constituents are unclear. In this study, we investigate the impact of terrestrial runoff on marine biogeochemistry in Inuit Nunangat (the Canadian Arctic Archipelago)—a key pathway for transport and modification of waters from the Arctic Ocean to the North Atlantic—using sensitivity experiments from 2002 to 2020 with an ocean model of manganese (Mn). The micronutrient Mn traces terrestrial runoff and the modification of geochemical constituents of runoff during transit. The heterogeneity in Arctic runoff composition creates distinct terrestrial fingerprints of influence in the ocean: continental runoff influences Mn in the southwestern Archipelago, glacial runoff dominates the northeast, and their influence co-occurs in central Parry Channel. Glacial runoff carries micronutrients southward from Nares Strait in the late summer and may help support longer phytoplankton blooms in the Pikiyasorsuaq polynya. Enhanced glacial runoff may increase micronutrients delivered downstream to Baffin Bay, accounting for up to 18% of dissolved Mn fluxes seasonally and 6% annually. These findings highlight how climate induced changes to terrestrial runoff may impact the geochemical composition of the marine environment, and will help to predict the extent of these impacts from ongoing alterations of the Arctic hydrological cycle.

Plain Language Summary In the Arctic, climate change is expected to increase river flow and alter the composition of river water through permafrost thaw and glacial melt. Many rivers and land areas drain to the coastal Arctic Ocean; the impact of changes to the nutrients carried by river water to these regions are unclear. In this study, we focus on Inuit Nunangat (the Canadian Arctic Archipelago)—a series of shallow channels that connects the Arctic Ocean to the North Atlantic—and look at where in the ocean the material in the river water ends up and how much of the material travels downstream. We use experiments with an ocean model from 2002 to 2020 and track an element found in river water: manganese (Mn), which is also an important nutrient in the ocean. While continental rivers mainly influence Mn in the southwestern Archipelago, glaciers influence the northeastern Archipelago and supply nutrients to Pikiyasorsuaq, one of the Arctic's most biologically active areas. Glaciers can contribute up to 18% to Mn transported downstream of Nares Strait seasonally and 6% yearly. Our findings highlight how climate related changes in the composition of river water impact the marine system of Inuit Nunangat and how these changes can funnel downstream.

1. Introduction

All components of the Arctic freshwater system are experiencing shifts as a result of human-induced climate change (Serreze et al., 2006; White et al., 2007). Almost half of the freshwater contributed annually to the Arctic Ocean originates from runoff (Haine et al., 2015) and this runoff is fed by catchment basins that stretch far south, transferring lower latitude changes to the high latitudes. River runoff integrates large-scale climatic changes over these basins and transmits them to the continental shelves and Arctic Ocean where the runoff delivers freshwater, heat, sediments, and nutrients (Holmes et al., 2013). Observed and forecasted changes to Arctic rivers include enhanced discharge (Feng et al., 2021; McClelland et al., 2006; Peterson et al., 2002), a shift toward a groundwater-dominated system (Walvoord & Striegl, 2007), increased sediment and organic carbon supply from permafrost thaw (Aiken et al., 2014; Spencer et al., 2015), and glacial melt (Bhatia et al., 2013). These changes will lead to altered geochemical signatures in rivers throughout the Arctic (Frey & McClelland, 2009). The long-term effects of these changes on ocean biogeochemical cycles, circulation patterns, and primary productivity are far

Writing – review & editing: S. E. Allen,
M. Colombo, P. G. Myers, K. J. Orians

from understood, but evidence suggests that they will have substantial impacts both in the Arctic Ocean (Carmack et al., 2016; Prowse et al., 2015) and downstream in the subpolar North Atlantic (Greene & Pershing, 2007).

Inuit Nunangat, or the Canadian Arctic Archipelago (CAA), is characterized by an abundance of rivers, many shallow channels, and extensive coastlines which modify the biogeochemical properties of water as it transits from the Arctic Ocean to Baffin Bay and the North Atlantic Ocean (e.g., Colombo et al., 2021; McLaughlin et al., 2004; Rogalla et al., 2022)—these properties make it an ideal place to study the influence of runoff on the Arctic marine environment. For the purposes of this paper we will refer to the region of study as the CAA. The CAA is also highly productive and home to the northern hemisphere's largest polynya: the Pikialasorsuaq or North Water polynya. A few large rivers such as the Mackenzie River, drain the North American continent, alongside many smaller rivers and streams that flow from the continent and islands into the channels of the CAA (Prowse & Flegg, 2000). These extensive freshwater systems form a recurrent feature along coastlines termed the Riverine Coastal Domain (RCD), which connects terrestrial and marine ecosystems (Carmack et al., 2015). Differences in seasonal hydrology, bedrock geology, catchment basin scales, and landscape processes drive the heterogeneity of the geochemical characteristics of rivers in the CAA (Alkire et al., 2017; Brown, Williams, et al., 2020; Colombo et al., 2019; Grenier et al., 2022). The majority of the CAA also has some form of continuous or discontinuous permafrost (Frey & McClelland, 2009), and glaciers cover its northeastern regions including Ellesmere Island and Baffin Island. With predicted increased terrestrial runoff in a future climate, the RCD may become more prominent and its composition will likely be altered (Carmack et al., 2015).

Over the last few decades, research efforts into the Arctic freshwater system have expanded (Bring et al., 2016) using a range of methods: direct and remotely sensed observations, modeling studies, and conceptual frameworks. Long time series of river discharge and composition measurements exist for the “big-6” Arctic rivers (the Mackenzie, Yukon, Yenisey, Lena, Kolyma, and Ob) from the Arctic Great Rivers Observatory (Arctic-GRO) and PARTNERS projects (McClelland et al., 2008, 2015). Other recent studies have expanded on this information by studying the composition of runoff from smaller rivers in the CAA (Alkire et al., 2017; Brown, Williams, et al., 2020; Colombo et al., 2019). In the coastal oceans, the small size of the band of river influence (generally less than 10 km) makes observations sparse (Carmack et al., 2015). Climate models have focused on predicting hydrological changes to rivers (Nijssen et al., 2001) and the impact of freshwater on the physical dynamics of the ocean (Lique et al., 2016). Feng et al. (2021) combined hydrologic modeling and remote sensing to produce an overview of pan-Arctic river runoff and Stadyk et al. (2020) improved hydrological modeling of runoff into Hudson Bay. Recent improvements in the resolution of models allow for more detailed experiments of the role of runoff on coastal ocean chemistry (e.g., Tank et al., 2012). Lagrangian modeling has been used to identify meltwater pathways from the Greenland Ice Sheet into Baffin Bay (Gillard et al., 2016). Remotely sensed chromophoric dissolved organic matter (CDOM) has also been demonstrated as a helpful tool for tracing riverine influence in the Arctic Ocean, however satellites observe only the surface signatures (Fichot et al., 2013) and are limited by sea ice cover. Several conceptual studies and syntheses (Brown, Holding, & Carmack, 2020; Carmack et al., 2016; McClelland et al., 2012) have established frameworks within which to understand anticipated and observed changes to rivers in the ocean context. However, despite all this progress, we lack quantification of the extent to which the marine environment is linked to terrestrial runoff and how ongoing environmental changes will alter this important freshwater input.

The impact of geochemical constituents in terrestrial runoff on the marine environment is not only a function of ocean dynamics, but also the chemical and biological processes that alter the composition of water during transit in the ocean. While model experiments tracing runoff with “dye” or measurements of the dissolved oxygen isotope ratio are able to identify terrestrial freshwater or meteoric water presence, these approaches do not account for the modification (change of oxidation state, removal) of geochemical constituents over time. Manganese (Mn) is a trace element and essential micronutrient (Sunda, 2012) with advantageous properties for tracing terrestrial runoff that incorporates information related to oxidation-reduction and removal of Mn. Dissolved Mn has a scavenged-type vertical distribution with maximum concentrations near sources and low background concentrations; this contrast allows it to be used as a tracer of inputs such as terrestrial runoff (Landing & Bruland, 1980; Middag et al., 2011). Oxidation removes dissolved Mn on the time scale of weeks to months (Bruland et al., 1994; Colombo et al., 2020, 2022; Rogalla et al., 2022; Sunda & Huntsman, 1994; Van Hulst et al., 2017) and as it undergoes reversible scavenging and sinking, it remains in the ocean surface up to a few years (Jickells, 1999; Kadko et al., 2019; Landing & Bruland, 1987; Shiller, 1997). This timescale of Mn presence in the surface ocean is conducive to studying the transport of geochemical constituents. The distribution of Mn also informs

runoff impacts on other lithogenic-derived elements in the Arctic Ocean such as iron (Fe). However, while Fe and Mn share sources, dissolved Fe oxidizes more rapidly in absence of organic ligands, hence the maximum distance of lateral transport of dissolved Fe may be more limited (Jensen et al., 2020; Landing & Bruland, 1987). The oxidation of Mn is largely controlled by microbes (bacteria and fungi) which enhance oxidation kinetics in aquatic environments (Hansel, 2017), in particular near the shelf break (Colombo et al., 2022). Lastly, we can use available Mn observations in the ocean to evaluate the model representation.

In this study, we aim to provide insight into the response of the marine environment to anticipated changes in terrestrial runoff, with a focus on the CAA. We trace terrestrial runoff with experiments from a regional Mn model (Rogalla et al., 2022) within a coupled ocean-ice regional model configuration centered on the CAA (Hu et al., 2018) alongside in situ observations of riverine trace metals collected during the Canadian Arctic GEOTRACES (GN02, GN03) cruises in 2015 (Colombo et al., 2019). We separate the runoff sources by type and use simulations from 2002 to 2020 to study the spatial extent of terrestrial freshwater influence on dissolved Mn within the CAA to identify regions most strongly impacted by climate induced runoff composition changes. Then, we consider the implications of runoff composition changes on the quantities of constituents transported downstream to Baffin Bay. The results presented here will help interpret the implications of observed changes to the composition of the Arctic terrestrial freshwater system on the ocean.

2. Methods

In this study, we use a passive tracer model of dissolved manganese (Mn) in the CAA (Rogalla et al., 2022), applied to ocean and ice dynamics from the Arctic and Northern Hemispheric Atlantic configuration (ANHA12; Hu et al., 2018) of the Nucleus for European Modeling of the Ocean (NEMO; Madec, 2008). First we describe the ocean model, then the Mn model.

NEMO is a three-dimensional hydrostatic ocean model that solves the primitive equations on the Arakawa-C grid with a free surface (Madec, 2008). The ocean is coupled to sea ice which is represented using the dynamic and thermodynamic Louvain-la-Neuve (LIM2) model with an elastic-viscous-plastic ice rheology (Bouillon et al., 2009; Fichefet & Maqueda, 1997). The ANHA12 simulations do not have a land-fast ice parameterization and so, ice velocities in Parry Channel are higher than observed (Grivault et al., 2018; Hu et al., 2018). Tides are also not included in the current version of the configuration and as a result, polynyas are not always well reproduced (Hughes et al., 2018).

The ANHA12 configuration of NEMO has a $1/12^\circ$ resolution horizontal grid with a pole in North America, so the resolution effectively corresponds to 2–3 km in Parry Channel. This resolution allows the model to resolve freshwater fluxes associated with coastal currents in the CAA (Bacon et al., 2014; Chelton et al., 1998). The vertical axis is represented by 50 depth levels with highest resolution at the surface (box thickness ranges from 1 to 454 m) and the bottom bathymetry is represented with partial steps. The ANHA12 open boundaries, in Bering Strait and at 20°S in the Atlantic Ocean, are forced with Global Ocean Reanalyses and Simulations data (Masina et al., 2017). The ocean surface is forced with 10 m hourly atmospheric data from the Canadian Meteorological Center's global deterministic prediction system (Smith et al., 2014). Terrestrial runoff is based on monthly climatology and around Greenland, runoff is enhanced for melt (Bamber et al., 2012; Dai et al., 2009). The river runoff datasets end in 2007, while the Greenland runoff continues to 2010. Afterward, the runoff forcing from the last year with available data is maintained. Near large sources such as the Mackenzie River, runoff input is remapped (volume conserved) along the shoreline in order to prevent negative salinity artifacts (Hu et al., 2019). This remapping does not significantly impact the larger spatial scales discussed in this paper.

The Mn model is calculated offline on a sub-domain of ANHA12 centered on the CAA (Figure 1a). The NEMO-TOP engine (Gent et al., 1995; Lévy et al., 2001) calculates the advection and diffusion of Mn based on 5-day averaged dynamics fields from a reference experiment of ANHA12 from January 2002 to December 2020. In addition, the Mn model incorporates parameterizations of the sources and sinks that control the distribution of dissolved Mn in the Arctic Ocean (Figure S1a in Supporting Information S1): runoff, sediment resuspension, atmospheric dust deposition, dust and sediment flux from sea ice, reversible scavenging, and sinking. The model parameterizations estimate dissolved Mn(II), dMn, and incorporate the indirect effect of lithogenic particles containing Mn through dissolution. Oxidized Mn(IV), oMn, is incorporated to estimate reversible scavenging. The Mn model was evaluated with observations of dissolved Mn in August–September 2009 and 2015 from the

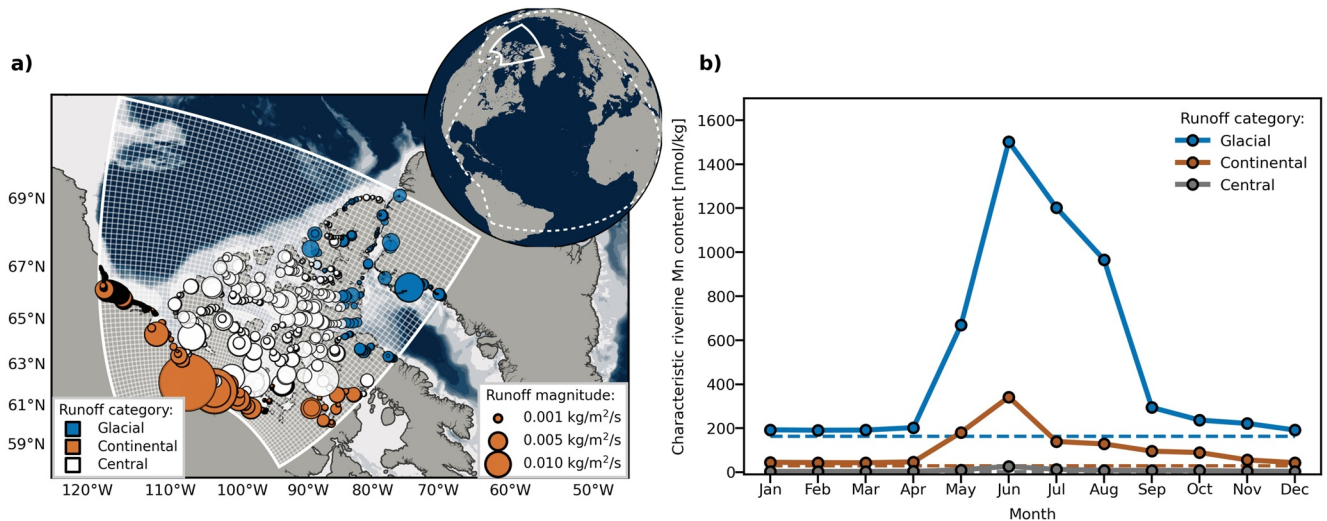


Figure 1. (a) Runoff sources in the model are grouped based on whether they drain glaciers (blue), the continent (brown), and central areas (white). The size of the markers is proportional to the discharge in September (scale indicated on the figure), 2010 from the ANHA12 model forcing (Bamber et al., 2012; Dai et al., 2009). Note that the runoff sources are remapped onto the model grid, sometimes across multiple cells (volume conserved) to prevent negative salinity artifacts (Hu et al., 2019). The dashed line on the inset globe corresponds to the full ANHA12 domain. The boundary of the ANHA12 sub-domain for the Mn model is indicated with a thick white line on both maps and the horizontal resolution of the grid is shown with a thin white line for every 10 gridpoints. The background shading represents the model bathymetry. (b) Mean characteristic Mn content, R_{class} (Equation 1), of all runoff sources in the domain. Dashed lines represent the base characteristic Mn content for each runoff type used by the “base”, “glacial”, and “continental” experiments. Solid lines indicate the seasonally varying Mn content projections based on Colombo et al. (2019), used for the “seasonality” experiment.

IPY and Canadian Arctic GEOTRACES (GN02, GN03) cruises (Colombo et al., 2020; Sim, 2018) and polar mixed layer concentrations from the 2015 US Arctic GEOTRACES GN01 section (GEOTRACES Intermediate Data Product Group, 2021; Jensen et al., 2020). The model performs well from deep regions in the Canada Basin to shallow areas in the CAA (Figure S1b-d in Supporting Information S1). It does not capture the full variability in near-bottom Mn increases and spatial variation in the magnitude of surface maxima, likely because of the low spatial and temporal resolution of available information for the strongly variable resuspension rates and sea ice sediment content. Here, we will describe the runoff Mn parameterization, since it is the focus of this study. For the full details of the Mn model, see Rogalla et al. (2022).

Terrestrial runoff including river discharge contributes Mn to the shelf seas and into the Arctic Ocean (Colombo et al., 2020; Middag et al., 2011). In our model, the dissolved Mn contributions depend on the seasonally fluctuating runoff, Q , and the dMn concentration of the runoff. Each runoff source is assigned a class, R_{class} , with associated dMn concentration based on its catchment basin (Figure 1a): if glaciers are present (“glacial”; cross-referenced with Natural Resources Canada, 2010) and if not, then whether the runoff drains the continent (“continental”) or the central islands (“central”). Observations of small CAA rivers by Colombo et al. (2019) suggest that glacial rivers have high concentrations of dissolved Mn, continental rivers have intermediate concentrations, and central rivers have low concentrations. The addition of dissolved Mn by runoff is estimated as:

$$\frac{\partial[dMn]}{\partial t} = \frac{Q}{\rho_0 \Delta z_{surface}} R_{class} \quad (1)$$

where ρ_0 is the density of freshwater ($1,000 \text{ kg m}^{-3}$) and $\Delta z_{surface}$ is the surface grid box thickness (1.05 m). In the base case, the dMn concentrations are assigned to R_{class} using observations from Colombo et al. (2019) in low flow conditions: 164 nM in glacial runoff, 30 nM in continental drainage, and 2 nM in central runoff. The dMn content for these categories falls within the lower end of the range of concentrations observed in the Kolyma, Severnaya Dvina, Ob, Lena, and Yenisey, and is comparable to those observed in the Mackenzie River (Hölemann et al., 2005; Holmes et al., 2013; McClelland et al., 2008; Pokrovsky et al., 2010). Our glacial dMn endmember concentration is on the upper end of the range of concentrations observed in runoff around Greenland (Hawkings et al., 2020; Van Genuchten et al., 2022).

Mn can also be indirectly added to the ocean by runoff through the photoreductive dissolution and desorption of Mn bounded to particulate matter. We chose not to include the particle-bound contribution of runoff, as we were

Table 1
Terrestrial Runoff Forcing Experiments Performed With the Mn Model

Experiment name	Description of runoff forcing ^a	Period
Base	Base Mn content classification	2002–2020 ^b
Glacial	Mn content in glacial runoff enhanced by 50%	2002–2020 ^b
Continental	Mn content in continental drainage enhanced by 50%	2002–2020 ^b
Seasonality	Seasonally varying Mn content in runoff	2002–2020 ^b

^aDischarge rates vary seasonally and are identical in all experiments. ^bPrior to the study period, the model is spun up by repeating the year 2002 three times.

unable to constrain the most representative contribution from suspended matter from the limited observations and since a larger portion of the particulate fraction is typically removed in estuaries (Gordeev et al., 2022; Rogalla et al., 2022). However, the Mn model does incorporate the indirect effect of lithogenic particle bound Mn on dMn from sediment resuspension and sediments in ice. Similarly, while there is clear evidence of the cycling of Mn in estuaries, we did not include this aspect in our study given the resolution of the model and the limited information available to quantify the necessary processes as this behavior varies strongly across regions and by season (Gordeev et al., 2022; Paucot & Wollast, 1997; Turner et al., 1991; Zhou et al., 2003). While the treatment of suspended matter and estuarine cycling present a limitation on the magnitude of Mn contributions, the spatial extent of impact is not significantly affected by changes to the contributions and our experiment with seasonally varying Mn in runoff gives an indication of the potential impacts of larger runoff Mn contributions. Unless explicitly stated otherwise, all following references to Mn are to the dissolved phase only.

2.1. Experimental Design

We performed four numerical experiments with the Mn model running from January 2002 to December 2020, altering only the terrestrial runoff Mn forcing (Table 1). Runoff discharge is identical in all experiments and varies seasonally, while the characteristic Mn concentration in runoff is constant in the “base”, “glacial”, and “continental” experiments and varies in the “seasonality” experiment. Each experiment is spun up by repeating the year 2002 three times, after which the year-to-year change in Mn profiles at evaluation stations is minimal (Figure S2 in Supporting Information S1).

We assess the impacts of changes to the Arctic terrestrial freshwater system on Mn in the ocean and their regions of influence by comparison with a “base case.” In the base case, we used the standard riverine Mn concentrations from observations in the CAA (Colombo et al., 2019). In the “glacial” experiment, we increased Mn concentrations in runoff draining glacial regions by 50% to emulate the increased contribution of micronutrients as a result of enhanced glacial melt (R_{class} in Equation 1). For the “continental” experiment, we increased Mn concentrations in continental runoff by 50% to emulate the increased contribution of trace metals from permafrost thaw and a stronger groundwater contribution. Although most rivers in the CAA drain permafrost covered areas, we chose to increase concentrations only in sources draining the continent, since these regions drain permafrost-covered catchment basins that extend southwards, and thus may see the greatest change in the near decades. In addition to the above experiments, we ran a “seasonality” experiment to look at the projected upper maximum seasonal runoff contribution to Mn. Using seasonal observations of discharge and Mn concentrations in the Kolyma river, Colombo et al. (2019) projected that Mn concentrations at peak flow could be up 1,280% those of low flow. In the “seasonality” experiment, we scale the Mn content in runoff so that at peak flow, concentrations are 1,280% the base concentrations and at low flow they are equal to the characteristic concentrations of the other experiments (Figure 1b). Mn observations in Colombo et al. (2019) were collected in August and we assume that this was during the low flow season. Note that the model runoff has not yet reached low flow in August, so the addition of Mn by runoff in August may be too high in the “seasonality” experiment.

2.2. Analysis

The Mn concentration at any cell is equal to the sum of contributions from all sources as the main equation defining Mn concentrations and distributions in the model is linear in Mn (Rogalla et al., 2022). We can separate the

contribution from a particular source with the difference between experiments. Here, we use the difference in Mn concentration between the “base” experiment and the experiments with a particular runoff type enhanced (“continental” and “glacial”) to calculate the percent that the specified runoff type contributes to Mn at a particular grid cell in the “base” experiment, P_{rt} (see Text S1 in Supporting Information S1 for derivation):

$$P_{rt} = \frac{Mn_{exp} - Mn_{base}}{Mn_{base}} \cdot \frac{1}{f - 1} \cdot 100\% \quad (2)$$

where f is the enrichment factor of the Mn runoff forcing in the experiment. We use $f = 1.5$ for a 50% increase in characteristic Mn concentration above the base case in the “continental” and “glacial” experiments. For the “seasonality” experiment, we calculate the percent difference relative to the base case and scale it by the enhancement factor (Equation 2) to isolate the impact of the seasonal variation of runoff concentration, not changes in magnitude. The enrichment factor is incorporated so that when P_{rt} is 100% at a particular grid cell, all the Mn in this cell is from the runoff type that was increased in this experiment. Anywhere that P_{rt} is non-zero, runoff from the type enhanced in that experiment is present in the ocean. The inverse is not-necessarily true—where P_{rt} is zero we can only say that Mn from runoff is not present (due to removal), not that there is no runoff present.

We can map P_{rt} for any other Mn runoff endmember concentration using the relation (Text S1 in Supporting Information S1):

$$P_{new} = \frac{f \cdot P_{rt}}{1 + \frac{P_{rt}}{100\%} (f - 1)} \quad (3)$$

where f is the ratio of the new Mn endmember concentration of a runoff type to the base Mn endmember concentration for that runoff type. When the change in endmember concentration is small, that is, $\frac{P_{rt}}{100\%} (f - 1) \ll 1$, the new percent contribution of runoff to Mn is nearly linear with the change in Mn endmember concentration and can be approximated as $f \cdot P_{rt}$. In areas with high P_{rt} (near coastlines) there is a nonlinear increase in P_{new} and a linear approximation would underestimate the new importance of the runoff type. While the magnitude of the contribution from runoff is altered by a change in Mn runoff endmember concentration, the overall spatial extent of influence of the runoff type will remain unchanged.

Transport of runoff-derived Mn was calculated across three main flow pathways from the Arctic Ocean toward the North Atlantic through the CAA: Nares Strait, Baffin Bay, and Parry Channel (boundaries in Figure 2a). The boundaries lie along lines of constant model grid i or j indices. The dMn flux, ϕ_{bdy} , is the sum of the dissolved Mn concentration at boundary grid cells with indices i, j, k , multiplied by the volume flux calculated from the velocity perpendicular to the boundary, u , and the grid cell area A :

$$\phi_{bdy}(t) = \sum_{i,j,k} [dMn]_{i,j,k}(t) \cdot u_{i,j,k}(t) \cdot A_{i,j,k} \quad (4)$$

where t is the time index of the 5-day averaged modeled velocity and Mn fields. Modeled fields were interpolated onto the U grid for the Baffin Bay and Parry Channel boundaries, and onto the V grid for the Nares Strait boundary. The boundary transports from the experiments were compared to the case with base runoff classification and the difference is represented as a percent (similar to Equation 2).

3. Results

Rogalla et al. (2022) found that within the CAA, resuspended sediments (40%–58%) and sediment released by sea ice (26%–37%) are the main external sources of dissolved Mn. Terrestrial runoff accounts for 5%–34% of external Mn addition across the CAA and is particularly important along coastlines and on regional scales. In this study, we investigate the influence of terrestrial runoff on the ocean in the CAA with experiments from the dissolved Mn model (Rogalla et al., 2022) developed with Mn observations from the rivers (Colombo et al., 2019) and the channels (Colombo et al., 2020). In our descriptions, terrestrial freshwater refers to river discharge and surface runoff from land in both glaciated and continental regions (as categorized in Figure 1a), and does not include the “central” runoff type whose influence on dissolved Mn is small as illustrated by the “seasonality” experiment. Glacial freshwater is supplied by glacial melt and rivers draining glaciated areas. Continental freshwater originates from rivers and surface runoff from the North American continent.

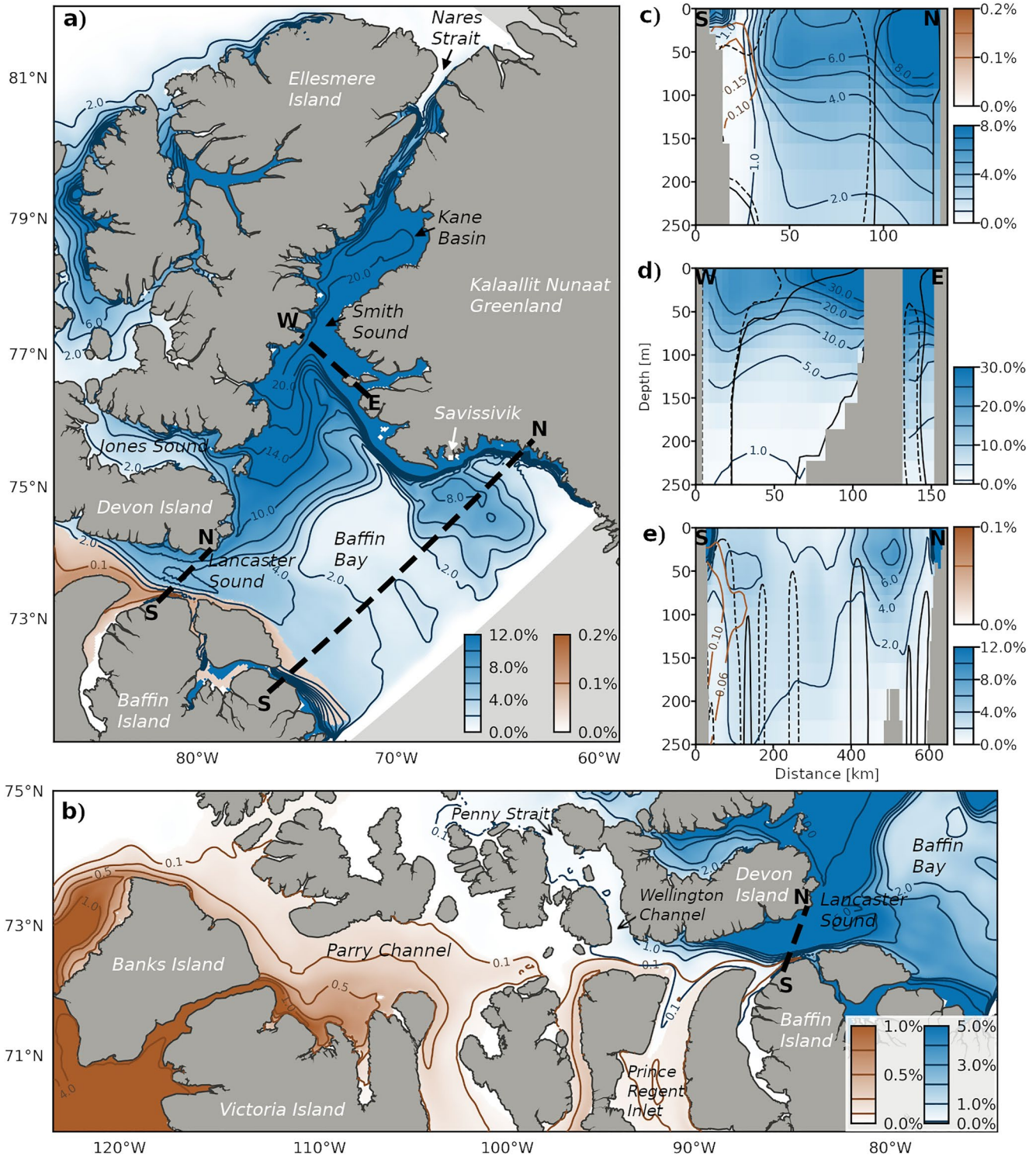


Figure 2.

3.1. The Spatial Extent of Glacial and Continental Runoff

Each type of terrestrial freshwater source in the CAA has a unique spatial fingerprint of influence as shown by Mn (dissolved; Figure 2). There is a distinct north-south separation between the continental and glacial runoff

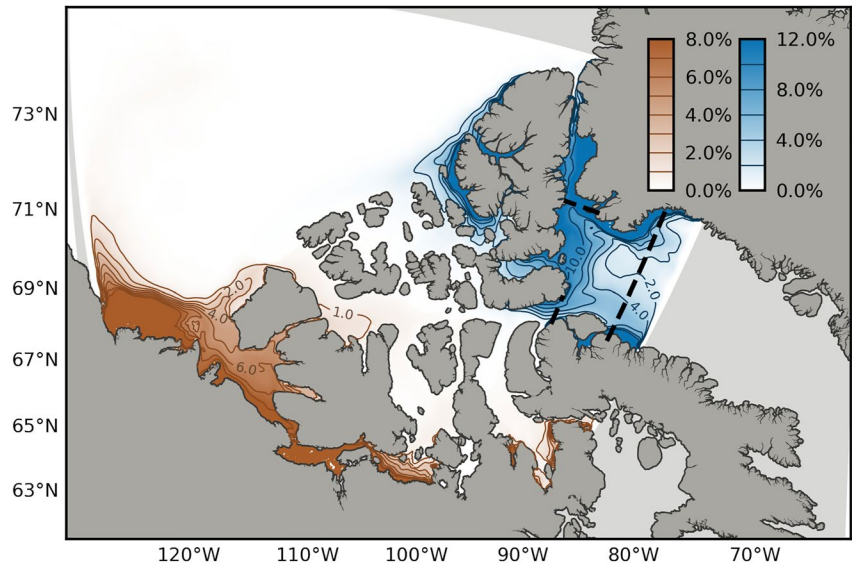


Figure 3. Continental (brown) and glacial (blue) terrestrial freshwater influence on Mn in the Polar Mixed Layer (upper 34 m of the water column) in the Canadian Arctic Archipelago, averaged from 2002 to 2020. The percent contributions are calculated as the increase of dissolved Mn in the continental and glacial enhanced experiments, relative to the base run (Equation 2). Where glacial and continental contributions overlap, the shading shows the component with greatest magnitude; contributions below 0.05% are masked. Regions outside of our sub-domain are colored light gray. Black dashed lines mark the locations of cross sections present in Figures 2c–2e and Figure 6.

influenced regions due to the geographic locations of the two types (Figures 1a and 3). In the following paragraphs, we describe these fingerprints and their overlap based on climatology from 2002 to 2020.

The “glacial” runoff sources affect inlets of the northwestern CAA, the coast of Baffin Island, and the Arctic waters transported through Nares Strait into Baffin Bay (Figure 2a), and the strongest contributions to Mn are found near coastlines. In Nares Strait, Mn from glacial runoff forms a band of >20% contribution along the Greenland coast and in Kane Basin. A plume extends from Kane Basin south through Smith Sound, where it separates from the Greenland coastal band (Figure 2d) and is entrained by the West Greenland Current. Runoff from Ellesmere Island extends predominantly westward along the continental shelf of the Canada Basin as marked by Mn. Along the east coast of Ellesmere Island, the near-shore contributions are lower (<8%) and are diluted by outflow from the Arctic Ocean. Across Baffin Bay (Figure 2e), the strongest glacial contributions to Mn (>15%) occur within 20 km of the coasts and down to 50 m depth, while a deeper and weaker glacial signature is visible toward the interior of Baffin Bay around 400 km from Baffin Island and originating from west of Savissivik on Greenland. Near Baffin Island, local glacial runoff sources contribute to a near shore maximum in Mn addition, while the influence from more distant Nares Strait outflow extends 200 km offshore and to 50–200 m depth (Figure 2e). Continental runoff from Parry Channel has a small additional contribution on Mn (<1%) at 20–250 m depth near the Baffin Island coast (Figure 2e).

Lancaster Sound, the gateway between Parry Channel and Baffin Bay, is influenced by both glacial and continental runoff as indicated by Mn distributions (Figures 2b and 2c). The prevailing direction of flow through Lancaster Sound is eastward (dashed black line in the cross section in Figure 2c) and this current transports Mn from continental runoff (the core extends from surface down to about 150 m) that originates from the southern

Figure 2. Continental (brown) and glacial (blue) terrestrial freshwater influences geographically distinct regions of the Canadian Arctic Archipelago as highlighted by the September climatological average of the runoff contributions to Mn in the upper 34 m of the water column for the northeastern Archipelago (a) and Parry Channel (b). These patterns are characteristic of the full model time period. See Figures S3–S7 in Supporting Information S1 for further detail on the spatial variation of continental and glacial runoff on Mn. Runoff contributions to Mn are calculated as the percent increase of dissolved Mn for the glacial and continental enhanced experiments, relative to the base run (Equation 2). Where glacial and continental contributions overlap, the shading shows the component with greatest magnitude (panels b–e); contributions below 0.05% are masked. Panel (a) has continental contributions plotted on top of glacial contributions to help visualize this component. We show the cross sections of continental and glacial runoff contributions to Mn in Lancaster Sound (c), Smith Sound (d), and Baffin Bay (e); boundaries are indicated with dashed black lines in panels (a) and (b). Dashed black contours in panels (c)–(e) represent volume fluxes in 2015 directed out of the page, while solid black contours are directed into the page (correspond to $400 \text{ m}^3 \text{ s}^{-1}$ for panels c–d and $2,500 \text{ m}^3 \text{ s}^{-1}$ for panel e).

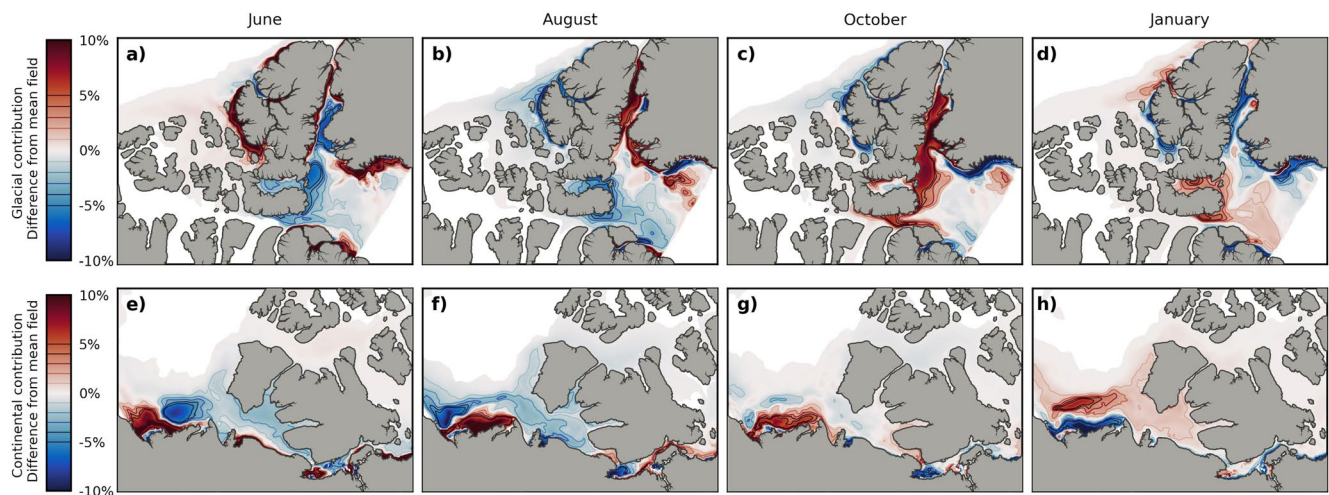


Figure 4. Snapshots of seasonal variations in the extent of glacial (panels a–d) and continental (panels e–h) terrestrial freshwater contributions to Mn in the Polar Mixed Layer (upper 34 m of the water column) in the Canadian Arctic Archipelago, based on monthly climatology from 2002 to 2020 calculated from the continental, glacial, and base experiments. The color bar indicates seasonal increases (red) and decreases (blue) in glacial (panels a–d) and continental (panels e–h) Mn contribution as a percent change from the mean field in Figure 3. Contributions smaller than 0.05% are masked.

CAA and recirculating glacial runoff that has spread to central Lancaster Sound toward Baffin Bay where they incorporate into the southward flowing Baffin Island current. Other sources such as sediment resuspension can also contribute Mn at these depths, which may be quite important (Rogalla et al., 2022). Nares Strait outflow and local sources from Devon Island contribute glacial runoff to the westward return flow in northern Lancaster Sound. This influence on Mn can reach as far west as Wellington Channel and extends well below 150 m. On the southern side of Lancaster Sound, local sources from Baffin Island contribute Mn in a shallow glacial band that extends 10 km offshore and to 30 m depth.

Continental runoff dominates the signature of Mn influence in the southern CAA and central Parry Channel (Figures 2b and 3). The largest continental river in our domain is the Mackenzie River, nearby the western boundary. The dominant direction of the Mackenzie River plume is eastward toward the CAA, however, strong westward wind events can drive the plume into the Canada Basin as evidenced by Mn distributions (Figure 5). The Mackenzie River plume Mn influence can extend over 400 km to the east of the river mouth and its effect is visible 200 km offshore. The highest continental contributions to Mn are found in the southwestern CAA (>10%). Overall, the continental runoff contributions to the Mn signature in the ocean are smaller and more diffuse than that of the glacial runoff. Continental runoff travels through Prince of Wales Strait and around Banks Island into central Parry Channel where the overall continental contributions of Mn are widespread and around 0.1%–0.5% (Figure 2b). The continental-origin terrestrial freshwater Mn extends north of Parry Channel in the northwest corner of the CAA for part of the year. The pathways of extension of continental runoff highlighted by Mn follow circulation pathways highlighted by pollutant dispersion experiments in Tao and Myers (2022).

While the overall north-south separation in Mn from continental and glacial origin freshwater is present throughout the year (Figure 3), there are month-to-month variations in the location and magnitude of contributions to Mn (Figure 4 and Figures S3–S4 in Supporting Information S1).

The seasonal variations in continental runoff contributions to Mn are most apparent on the Beaufort Shelf and in Parry Channel (Figure 4 and Figure S4 in Supporting Information S1). The Mackenzie River drives continental runoff on the Beaufort Shelf and dominates all other continental runoff sources (Figure 5). The minimum offshore extent of the continental contribution to Mn, 150 km, occurs in July and August. Starting in October and throughout the winter, continental runoff is pushed offshore. These months are associated with westward wind events that drive upwelling on the shelf and offshore transport (Stegall & Zhang, 2012). Continental runoff Mn contributions reach a maximum extent, 375 km offshore, by March. During the winter months (December to March), western Parry Channel also retains a weak but increased signature of Mn from continental runoff.

Glacial runoff contributions vary seasonally around Ellesmere Island, the Greenland coast, Nares Strait, Lancaster Sound, and in Baffin Bay as shown by Mn distributions (Figure 4 and Figure S3 in Supporting Information S1).

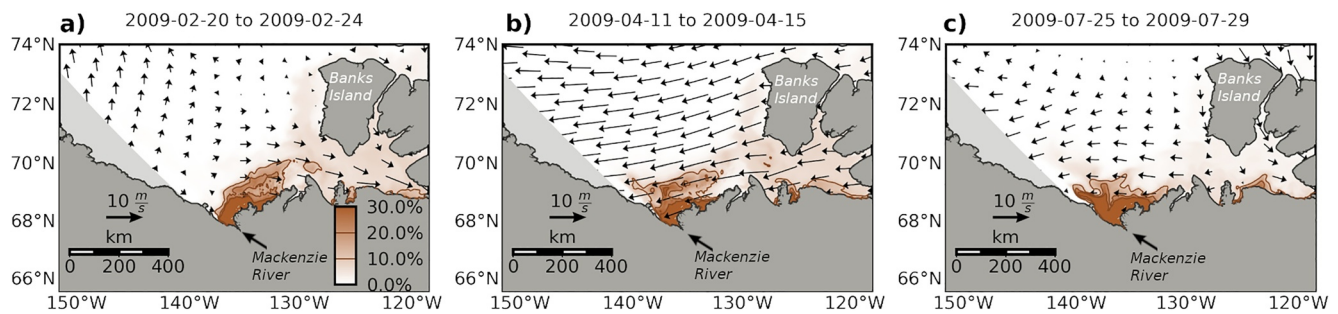


Figure 5. The Mackenzie River dominates continental runoff contributions along the Beaufort Shelf and the plume direction is affected by wind forcing as demonstrated through contributions to Mn in three five-day example periods in 2009 (panels a–c). Runoff contributions to Mn are calculated as the percent increase of dissolved Mn in the “continental” experiment, relative to the base run for each 5-day period (Equation 2) and averaged over the upper 34 m of the water column. Arrows indicate wind direction and speed at 10 m above the ocean based on the Canadian Meteorological Center’s global deterministic prediction system (Smith et al., 2014), averaged over the dates specified.

Runoff contributions to Mn extend from Ellesmere Island along the northwest coast 100 km offshore from December through May. During these months, runoff contributions to Mn in Nares Strait are diminished due to a combination of low discharge rates and strong Arctic Ocean inflow. Starting in June, we see strong coastal increases in glacial contributions to Mn along western Nares Strait and in the following months, central Nares Strait receives strong contributions from both Greenland and Ellesmere Island. In September, more of the Nares Strait runoff contributions extend southward into Baffin Bay as marked by Mn. Runoff influence on Mn concentrations from the coast of Greenland along Baffin Bay is strongest March through June. The main impact patch separates from the cape near Savissivik and is transported into Baffin Bay from June to August (signature present in September–October as well; Figure 2a, Figure S3f–h in Supporting Information S1). From October through February, the contribution of glacial runoff on Mn extends into northern Lancaster Sound and in October and November extends from the North side to the central and southern part of Lancaster Sound (Figure 4). Local Baffin Island glacial runoff contributions to Mn are strongest from May to July and remains near the Baffin Island coast.

3.2. Time Series of Runoff Contributions to Mn Transport Through Main Pathways

Time series of fluxes of Mn (dissolved) are calculated across three main cross-sections from the Arctic Ocean to the North Atlantic through the CAA: Nares Strait, Baffin Bay, and Parry Channel (Figure 6 and Figure S8 in Supporting Information S1; boundaries in Figure 2a). We compare the transports calculated from the sensitivity experiments relative to the base run following Equation 2. The physical dynamics and discharge rates are the same for all experiments, so any differences are indicative of a change in supply. Interannual variations are associated with changes in routing.

There are no strong temporal trends in runoff contributions to Mn (dissolved) outflow between 2002 and 2020 (Figures 6d–6f). Note that the runoff forcing after 2010, repeats the year 2010, so any changes from 2010 to 2020 are related to transport differences instead of supply. A gradual increase in glacial contributions to Mn is apparent in Nares Strait from 2002 to 2014 (Figure 6d). Similarly, although small in magnitude, the glacial contributions to Mn transport through Parry Channel increase from 1.5% in 2003 to 2.4% in 2014 and remain constant from 2014 to 2020. Throughout the time series, continental runoff contributions to Mn are negligible across the Parry Channel, Baffin Bay, and Nares Strait boundaries, relative to glacial contributions (Figure 6). Continental runoff typically contributes around 0.05% to Mn outflow at Parry Channel and Baffin Bay. The greatest continental contributions to Mn transport occur in Parry Channel (up to 0.2%) in December 2004, 2017, and 2019, with coincident increases in the Baffin Bay outflow.

Runoff contributions to Mn outflow are most important for Nares Strait, with glacial runoff contributing 4%–6% and varying strongly seasonally (Figures 6a and 6d). Glacial runoff contributions to Mn are greatest in September–October reaching up to 18% about 3 months after peak runoff, and drop to around 2% in March–May (Figures 1b and 4c, Figure S3 in Supporting Information S1). Southward glacial Mn transport through Baffin Bay is greatest in July in 2002–2005, just after peak runoff and prior to the peak in Nares Strait outflow as indicated by Mn fluxes (Figures 6a and 6b). The seasonal cycle of runoff contributions to Mn in Baffin Bay is less coherent from 2006 to 2020 (Figure 6b). The cumulative contribution of glacial runoff to Mn transport in Baffin Bay is around 2.9% (Figure 6e).

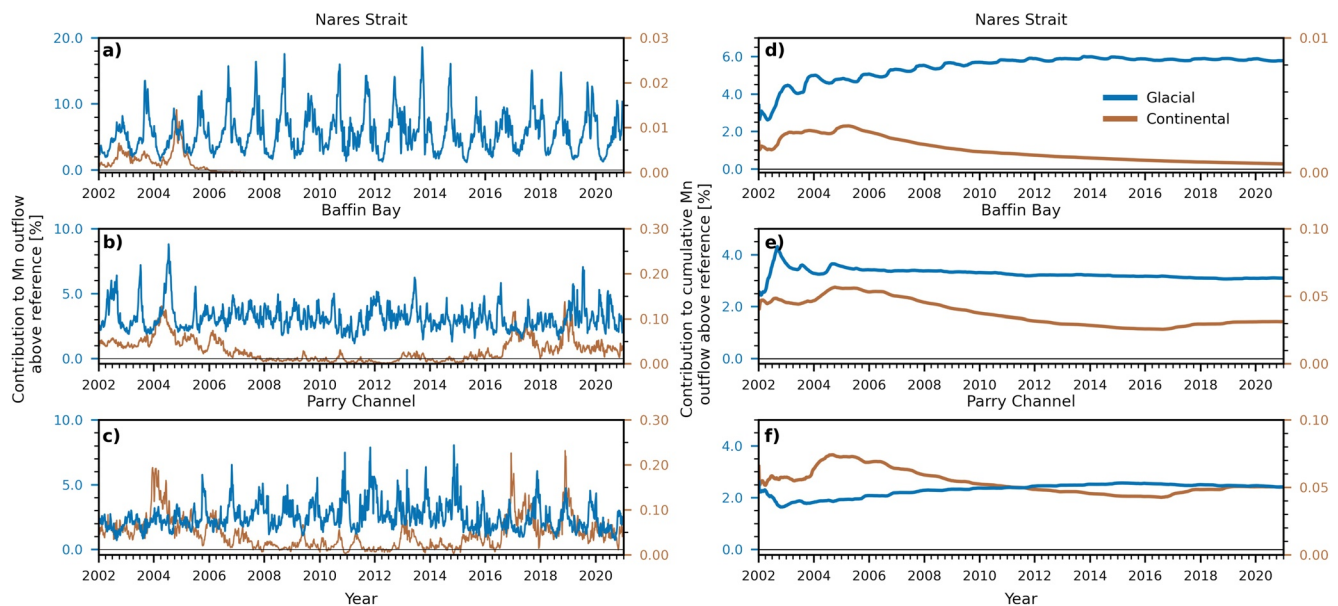


Figure 6. Time series of instantaneous (panels a–c) and cumulative (panels d–f) enhanced Mn (dissolved) outflow (eastward and southward) in glacial melt (blue) and permafrost thaw (brown) experiments at important flow pathways (boundaries shown in Figure 2a). Fluxes are calculated over the full water column from 5-day velocity and tracer fields and compared with the base run (Equation 2). Glacial and continental runoff Mn contributions vary seasonally (scaled time series in Figure S11a–S11c in Supporting Information S1). The contribution of each runoff source to cumulative Mn outflow is calculated as the cumulative sum over time of the Mn flux in the glacial (or continental) experiment relative to the total Mn flux from the base run. Note the different vertical axis scales between experiments and panels (axes labels are colored to indicate which component they present).

Runoff contributions to Mn flux at Parry Channel are lower than at the other boundaries (Figures 6c and 6f). This difference is likely driven by the relative distance of this boundary from strong Mn runoff sources, as oxidation and sinking of Mn removes contributions, and the importance of other sources of Mn. Instantaneously, glacial contributions to Mn transport typically range from 1% to 3% with some strong seasonal peaks up to 8% (Figure 6c). Higher glacial contributions to outflow from Parry Channel are seen in October with Mn distributions; the months where Nares Strait glacial runoff extends into Lancaster Sound (Figure 4 and Figure S3 in Supporting Information S1).

3.3. Impact of Seasonally-Varying Content of Runoff

Trace element concentrations in Arctic rivers vary seasonally with discharge as snow melt flushes top-soils during the spring freshet (Bagard et al., 2011; Hölemann et al., 2005). Observational time series of riverine Mn are lacking in the CAA, however Colombo et al. (2019) estimated an upper bound on potential concentrations using the Kolyma river as a proxy. Our “seasonality” experiment incorporates this information into an alternate runoff forcing where dissolved Mn concentrations at peak flow are 1,280% of those during the low flow season (Figure 1b). The monthly variations in the spatial extent of runoff influence on Mn are similar between the experiments with constant Mn concentrations in runoff (“base”, “continental”, and “glacial”) and the “seasonality” experiment (Figure 4 and Figure S3-7 in Supporting Information S1). The proportion of contributions to Mn in the mean field are also comparable (Figure 3 and Figure S5 in Supporting Information S1). These similarities are indicative of the importance of the freshet in controlling the spatial distribution of runoff. Differences between the extension of runoff influence on Mn in Figure 4 compared to Figure S6-7 in Supporting Information S1 highlight seasonal variations in flow pathways. Runoff contributions to Mn during low flow season appear lower in the seasonality experiment (Figures S3-4, S6-7 in Supporting Information S1), however this is an artifact from the normalization based on the 1,280% increase at peak flow (f in Equation 2). The overall oceanic influence of runoff on Mn scales proportional with the increase of concentrations in runoff associated with peak discharge, however the magnitude is not exactly 12.8 times the estimates from the base run (Figure 6 and Figure S8 in Supporting Information S1). The seasonal cycle of Mn transport across the boundaries is more pronounced in the “seasonality” experiment, however the timing of extrema is unchanged (Figure S8 in Supporting Information S1).

4. Discussion

Rivers connect terrestrial and marine ecosystems, conveying water, heat, sediments, carbon, and nutrients to the coastal domain and eventually into the ocean. The magnitude and composition of this terrestrial runoff is changing—the hydrological cycle is accelerating and landscape processes along the river catchment basins are being altered (Feng et al., 2021; Frey & McClelland, 2009). In the Arctic, permafrost thaw and glacial ice melt will have increasingly prominent effects on terrestrial runoff composition (Aiken et al., 2014; Bhatia et al., 2021; Koch et al., 2013). These riverine changes have cascading impacts on the ocean, reinforcing the need to identify the oceanic regions most directly impacted by this terrestrial runoff. In this study, we alter runoff input of dissolved Mn from glacial and continental permafrost draining regions in the CAA in a model to identify oceanic regions most affected by changes and we estimate fluxes of dissolved Mn downstream to Baffin Bay. These findings will facilitate the interpretation of biogeochemical observations collected in the coastal CAA and could help better predict the implications of observed basin scale runoff changes.

4.1. Charting the Terrestrial Fingerprint of Runoff on the Ocean

River discharge is transported in the ocean via coastal-trapped, buoyancy driven boundary currents (Münchow & Garvine, 1993). In the Arctic Ocean, these boundary currents flow with landmasses to the right and their width is typically 5–10 km (Rossby radius). The contributions from the many freshwater point sources merge and form the RCD (Carmack et al., 2015; Simpson, 1997; Vannote et al., 1980) that extends along the coastline. Our results effectively visualize the RCD extent by describing the fingerprints of influence of continental and glacial runoff on Mn in the ocean in the CAA and on the Beaufort Shelf. First, we compare our simulated terrestrial freshwater Mn extents with hydrographic observations and remotely sensed studies to establish the facilities of the model and this approach. Then, we discuss the seasonal variation and drivers of the extent of influence of terrestrial runoff on the ocean in the CAA using Mn.

The extent and variability of continental runoff identified in this study using Mn is comparable to hydrographic observations in the Canada Basin from 2010 to 2012 (Shen et al., 2016) and remotely sensed dissolved organic matter distributions from August 2002 to 2009 (Figures 4 and 5; Fichot et al., 2013). The concentration of Mn in continental runoff in the base run falls within values reported by the PARTNERS program (McClelland et al., 2008). In our model, the interior of the Canada Basin is relatively isolated from runoff and has low concentrations of river-derived nutrients (Figure 3; Shen et al., 2016). Continental runoff from North American rivers extends along the Beaufort Shelf as illustrated by Mn and is dominated by the Mackenzie River plume (Figure 5; Yamamoto-Kawai et al., 2010). The Mackenzie River plume generally extends eastward toward the CAA, however, it travels westward episodically (Figure 5; Yamamoto-Kawai et al., 2009). Samples of dissolved organic carbon (DOC), CDOM, and oxygen isotope composition collected between 2010 and 2012 also indicate westward Mackenzie River extent (Shen et al., 2016, sampling did not extend to the east of the Mackenzie River). An increase in the frequency of events that direct Mackenzie River water westward could contribute to an increase in the freshwater content of the Canada Basin (Fichot et al., 2013). However, during our time series, we did not identify an increase in the frequency of the extension of Mackenzie River runoff into the central Canada Basin using Mn as a tracer of these inputs.

Within the CAA, the RCD is dominated by many local point sources that combine, rather than a few large rivers. In our simulations, Mn from continental runoff is prevalent in the southern CAA, while Parry Channel receives weaker runoff contributions of Mn (Figure 2) due to the lack of large river systems as are found on the continent. These patterns are similar to those identified by barium and salinity measurements (Yamamoto-Kawai et al., 2010). As the distance from the source location increases, the terrestrial freshwater influence on Mn extends deeper in the water column and is weaker, likely through a combination of processes affecting Mn such as oxidation and removal by sinking, and physical processes such as mixing (Figures 2c and 2e). Buoyancy boundary currents have been identified on both sides of channels in the CAA combining hydrographic data and traditional knowledge (Arfeuille, 2001). Our results indicated bands of runoff on both shores of Lancaster Sound as traced by Mn (Figures 2a and 2c). On the north end of Lancaster Sound, a coastal current from Baffin Bay recirculates (Prinsenberget al., 2009; Tao & Myers, 2022; Wang et al., 2012) with strong contributions of Mn from glacial runoff in our study, particularly during late summer months (Figure 4c). This glacial runoff also appears in observations of trace metals and satellite imagery of this region (Colombo et al., 2020, 2021). In addition to direct glacial discharge, sub-glacial plumes can entrain nutrients from deeper water (Bhatia et al., 2021);

the model spatial resolution is not large enough to resolve entrainment at the glacier mouth. However, Bhatia et al. (2021) identified that sub-glacial plumes predominantly entrain macronutrients while micronutrients such as Fe and Mn originate from the surface glacial discharge which our model includes. The south end of Lancaster Sound, near Baffin Island, is relatively fresh with an increased meteoric water contribution based on its oxygen isotope composition (Yamamoto-Kawai et al., 2010) and in our study received Mn primarily from local glacial freshwater and weaker contributions from continental freshwater outflow from the CAA (Figure 2).

In some strong mixing regions of the CAA, Mn from terrestrial freshwater extends further than advection alone can account for. In western Parry Channel, Mn from continental freshwater extends northward counter to the prevailing flow directions (Figure 2b) and in central Parry Channel, the westward Lancaster Sound return flow supplies glacial freshwater (and Mn) to Wellington Channel where a small portion travels northward into Penny Strait (Figures 2b and 4c). These extended ranges of influence appear in regions associated with strong tidal mixing. While the model configuration used in this study does not have tides, the model reproduces the locations of these mixing hot-spots (Hughes et al., 2017) and thus they could contribute to this extension in Mn from terrestrial freshwater. Sediment resuspension in the Mn model is also stronger in regions with high tidal stresses, but does not impact our estimate of Mn from runoff in these areas as the sediment resuspension is identical in all experiments.

Seasonal variations in the extent of terrestrial freshwater and Mn in the ocean are affected by the runoff discharge rates. River discharge peaks during the spring freshet, typically starting in mid-May and extending to June or July in the CAA (Alkire et al., 2017; Li Yung Lung et al., 2018). The characteristic Mn content of runoff during the freshet sets the magnitude of Mn contributions from runoff to the ocean, as indicated by the increase in oceanic contributions roughly proportional to the concentration at peak discharge in the “seasonality” experiment (Results Section 3.3). In the “seasonality” experiment, runoff contributions to Mn transport across the boundaries are about half the magnitude of transport in the “glacial” and “continental” experiments when scaled by the Mn content of runoff at peak discharge (Figure S8 in Supporting Information S1). This difference suggests that the freshet may contribute about half the annual Mn transport across the boundary, in agreement with estimates that 57% of annual discharge occurs during the time period including the freshet from April to July (Lammers et al., 2001; Li Yung Lung et al., 2018). During the spring freshet, freshwater accumulates along coastlines as illustrated by Mn distributions and can form a strong frontal structure that separates the nearshore and offshore (Figures 4a, 4e, and Figure S5-6 in Supporting Information S1; Moore et al., 1995). From September to April runoff is lower (Figure 1b), the nearshore of the Beaufort Shelf has a weakened continental freshwater contribution of Mn, and runoff accumulated during the summer season is transported offshore (Figures 4g and 4h). Where runoff ends up in the ocean is affected by the timing of the freshet, so the observed shift toward an earlier freshet and an increase in fall discharge could impact the oceanic distribution of constituents of runoff such as Mn (Ahmed et al., 2020).

The redistribution of terrestrial freshwater in the ocean depends on sea ice, winds, and ocean currents, all of which vary seasonally (Macdonald et al., 1995). In our climatology, the freshwater contributions to Mn in Nares Strait, Lancaster Sound, and over the Beaufort Shelf remained confined to the nearshore during the summer and spread offshore in the winter months (Figure 4 and Figure S4 in Supporting Information S1). The offshore transport is affected by the sea ice extent and the mobility of sea ice (Figure S10 in Supporting Information S1). When sea ice is mobile, wind stress is transferred more directly to the water column (Pickart et al., 2009), while immobile ice tends to widen buoyancy boundary currents because of increased surface-stress from flow beneath the ice (Ingram, 1981; Kasper & Weingartner, 2015). During winter months with full sea ice coverage, signatures of continental and glacial runoff on Mn contributions are redistributed offshore from the Beaufort Shelf and the northwest coast of Ellesmere Island (Figures 4c and 4d and Figures S9-10 in Supporting Information S1). In Nares Strait, freshwater distributions are also controlled by the strong ocean currents. An August reduction in sea ice thickness coincides with the spread of freshwater influence on Mn into central Nares Strait. The subsequent extension southward in September-December occurs in low-sea ice conditions and follows the Lancaster Sound return flow and geostrophic flow eastwards into Baffin Bay and the southward flowing Baffin Island current (Figure 4b and Figures S3 and S6 in Supporting Information S1). Wind can also direct plumes of runoff within the ocean. As described in Macdonald et al. (1995), in our “continental” experiment, the Mackenzie river plume traced by Mn spreads toward the shelf-break as sea ice retreats (Figure 4e-4f and Figure S10 in Supporting Information S1). Without sea ice coverage, winds can directly push and separate the Mackenzie runoff plume from the coast of the Beaufort Shelf (Figure 5; Mulligan & Perrie, 2019). Based on observations, these winds act to divert

the plume on timescales of less than a day and can push the plume offshore by up to 30 km per day (Mulligan & Perrie, 2019).

While our model does not represent estuarine dynamics and has a resolution of a few kilometers, when compared with hydrographic and remotely sensed observations, the model represents the overall flow structure of runoff in the ocean on the extensive spatial scale of this study. We discussed the spatial variations of terrestrial freshwater signatures illustrated by Mn distributions (Figures 2 and 3) and the drivers of runoff extent in the CAA and the resulting seasonal variations in influence (Figure 4). Both the spatial variations and seasonality of terrestrial freshwater input have direct consequences on the biology and geochemistry of the Arctic Ocean (Brown, Holding, & Carmack, 2020).

4.2. Glacial and Continental Runoff Supply Micronutrients Directly to the Pikialasorsuaq North Water and Cape Bathurst Polynyas

Glacial and continental runoff feeds micronutrients to the ocean and could thereby affect the magnitude and seasonal cycle of phytoplankton blooms, in particular with enhanced contributions from glacial melt and permafrost thaw (Aiken et al., 2014; Bhatia et al., 2013, 2021; Spencer et al., 2015). As illustrated by dissolved Mn distributions, terrestrial freshwater influence is present in our domain in areas with polynyas (Hannah et al., 2008) including the well-known Pikialasorsuaq or North Water polynya (PNOW) in northern Baffin Bay and the Cape Bathurst polynya on the Beaufort shelf (Figures 3 and 7). These polynyas are associated with high levels of primary productivity which in turn supports a large biomass of zooplankton (Saunders et al., 2003), fish, and marine mammals including belugas, narwhals, and bowhead whales in the Pikialasorsuaq (Heide-Jørgensen et al., 2013), and an abundance of ringed seals in the Cape Bathurst Polynya (Harwood & Stirling, 1992). The productivity is controlled by the hydrographic and geochemical characteristics of the water which is a function of basin-scale circulation and local inputs from land (Bring et al., 2016; Mei et al., 2002). In our simulations with Mn, the PNOW is directly impacted by glacial runoff that originates from Greenland and Ellesmere Island via Nares Strait, while the Cape Bathurst polynya receives continental runoff downstream of the Mackenzie River (Figures 3 and 7). For the following discussion, note that the ANHA12 simulation captures the shape of the PNOW polynya and also simulates the weaker advection of sea ice at Smith Sound and to its south, however the period of ice cover is longer in the model (Hu et al., 2018).

While the start date of the spring bloom in the PNOW is largely controlled by light availability through the retreat of sea ice, nutrients supplied by freshwater runoff sources, such as glacial melt, could help support longer bloom duration. The longest climatological bloom estimated from satellite chlorophyll-a records from 1998 to 2014 was around 106 days and occurred in Smith Sound, along the Greenland Coast (off Kane Basin) and toward Jones Sound (Marchese et al., 2017). These locations have the earliest bloom start dates, lowest sea ice concentrations, and highest bloom amplitudes (Figure S9 in Supporting Information S1; Marchese et al., 2017). Our Mn model also indicates that these locations receive some of the strongest contributions from glacial runoff during the summer months (Figure 7). Specifically, in Smith Sound and central Kane Basin, glacial runoff contributes

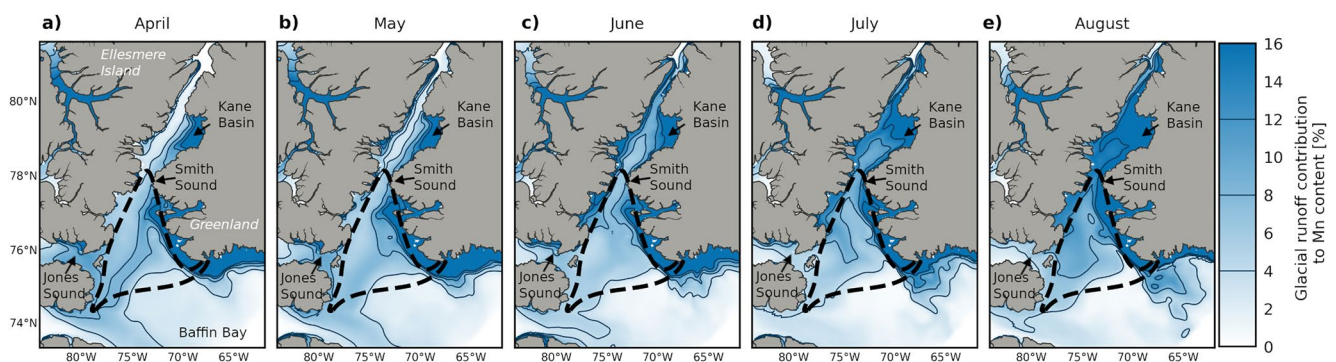


Figure 7. Glacial runoff extends to highly productive regions in Nares Strait as traced by Mn distributions. Panels a–e are climatological monthly glacial runoff contributions to dissolved Mn in the upper 34 m of the water column in the region of the Pikialasorsuaq or North Water polynya, delineated by the dashed black line, from April to August. The contributions are calculated from the “glacial” and “base” experiment (Equation 2) and averaged monthly between 2002 and 2020. Contour lines mark every 4%.

8%–18% to Mn concentrations from June through August, when nutrients typically become limiting and dinoflagellates replace diatoms (Lovejoy et al., 2002; Tremblay et al., 2002). We see notable glacial inputs along the Greenland coast throughout the summer season. The geochemical signature of glacial melt has been shown to be high in macronutrients such as nitrate and micronutrients such as Fe and Mn, and its supply could thus support productivity (Bhatia et al., 2013, 2021). Buoyancy-driven upwelling induced by sub-glacial discharge from marine-terminating glaciers could also contribute to higher macronutrient load (Bhatia et al., 2021).

A decline in the overall primary production has been observed in the PNOW over the last couple of decades and suggested causes include large-scale changes in the Arctic Ocean such as freshening, warming, or increased stratification, and local scale forcing changes such as surface winds and nutrient supply (Bergeron & Tremblay, 2014; Blais et al., 2017; Marchese et al., 2017). The nutrient inventory of the outflow from the PNOW is also a matter of interest since it is likely to affect the productivity in northern Baffin Bay (Tremblay et al., 2002). In our model simulations, we did not see a significant long term trend in Mn transport out of Nares Strait across the Smith Sound region from 2002 to 2020 and the composition of this transport also did not significantly change: the total annual glacial Mn transport across the Nares Strait boundary remained relatively constant (Figure 6d). The sources and sinks of Mn in the model vary with time (except for resuspension), however the runoff forcing after 2010 maintains that year. Hence a reduction in glacial runoff supply from 2010 to 2020 due to alternate routing is unlikely to contribute to the observed decline.

4.3. Local Changes to Runoff in the Canadian Arctic Archipelago May Alter the Biogeochemical Composition Downstream in Sub-Arctic Seas

The CAA accounts for about a third of freshwater export from the Arctic Ocean to the North Atlantic (Haine et al., 2015); a close second to the major outflow through Fram Strait in combined liquid and solid freshwater export. As waters transit through the shallow CAA, their composition is altered through strong shelf-ocean interactions and contributions from many runoff sources (e.g., Colombo et al., 2021). As such, changes to runoff composition and supply within the CAA can alter the geochemical and nutrient composition of the CAA outflow, and influence biogeochemical composition downstream in Baffin Bay, the Labrador Sea, and eventually the sub-polar North Atlantic. We estimated glacial and continental runoff contributions to dissolved Mn fluxes through the main channels of outflow from the CAA: Parry Channel and Nares Strait, and across Baffin Bay (Figure 6). With these fluxes, we highlight the importance of glacial runoff to Mn distributions and use Mn to estimate how long it takes for glacial and continental runoff changes to feed downstream (Figure 8).

Runoff released during the spring freshet can take several months to reach key channels such as Nares Strait, Parry Channel, and Baffin Bay, depending on travel distance and routing (Figure 8 and Figure S11 in Supporting Information S1). Runoff constituents with geochemical cycling, like Mn, undergo time-dependent scavenging and removal during transit, and so transit times affect the potential of runoff to alter the biogeochemical composition downstream. We estimated the transit time as the difference annually between the peak source discharge and peak runoff contribution to Mn in the boundary Mn flux time series (Figure 6 and Figure S11 in Supporting Information S1). In Nares Strait, glacial contributions of Mn to Mn outflow typically peak around 99 days after peak discharge (i.e., September), when a plume of glacial runoff extends southward from Nares Strait (Figure 2a and Figure S5i in Supporting Information S1). The distribution in arrival times in Nares Strait is more tightly constrained than in other passageways (Figure 8a). In Baffin Bay, glacial runoff traced by Mn arrives from local sources on Baffin Island and Greenland, from upstream areas such as Nares Strait, and through recirculation from Parry Channel (Figure 2; Gillard et al., 2016); this diversity in source regions is reflected in the broad range of arrival times and a typical arrival time shorter than Nares Strait at 74 days (Figure 8a). For Baffin Bay, local sources from Baffin Island and Greenland may be more important in determining the peak Mn runoff fluxes than Nares Strait outflow. Parry Channel glacial fluxes peak later than the Nares Strait and Baffin Bay maxima as a result of the late season arrival of Nares Strait glacial runoff via the Lancaster Sound return flow (Figure 4c).

The continental freshet typically takes around 110 days to reach Baffin Bay and Parry Channel (Figure 8b, S11e-f in Supporting Information S1), but can take over 200 days, suggesting more potential for removal of geochemical constituents before reaching Baffin Bay compared to glacial runoff. The broad ranges in the continental runoff arrival time in Parry Channel and Baffin Bay likely reflect the larger distance between major runoff sources, such as the Mackenzie river, and the Parry Channel and Baffin Bay boundaries (Figure 3). However, the broad range may also be due to the relatively weaker seasonal signal in boundary Mn fluxes (Figure S11a-c in Supporting Information S1) and the associated smaller number of peaks included in the arrival time estimate. The length of

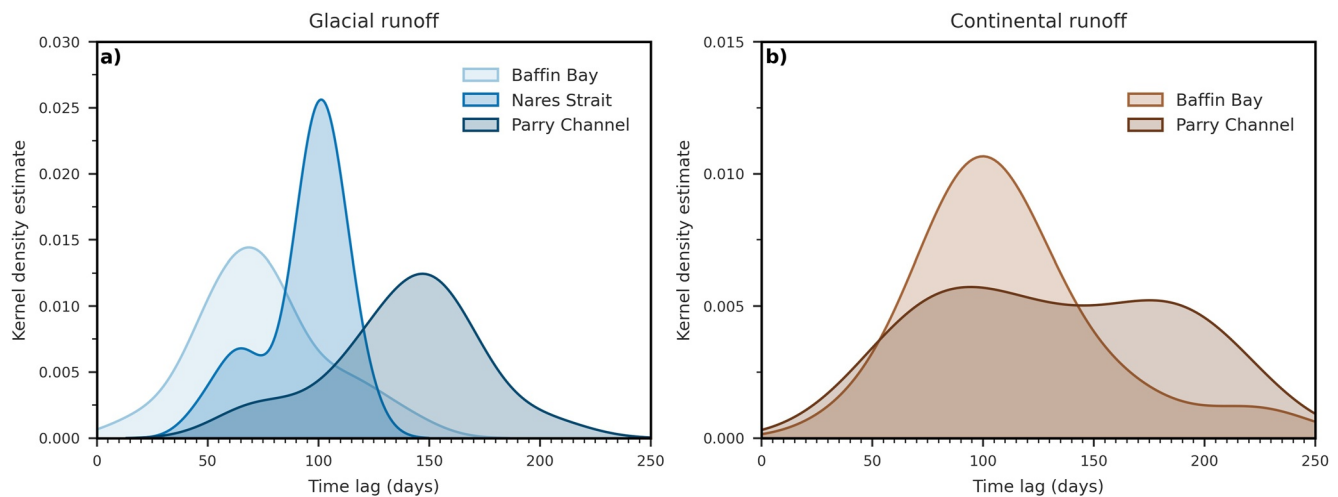


Figure 8. Runoff contributions to downstream dissolved Mn fluxes across key channels in the Canadian Arctic peak after the spring freshet. The time lag of the arrival of this maximum depends on the travel distance and route between the runoff sources and the boundaries. We calculated the kernel density estimates of the transit time between peak discharge and peak Mn flux from runoff for the (a) glacial and (b) continental runoff, based on the time series in Figure 6a–6c and and Figure S11 in Supporting Information S1 (boundaries marked in Figure 2a).

the continental and glacial freshet is comparable in the model forcing (Figure 1b), so the forcing is unlikely to contribute to the spread in arrival times.

Glacial runoff contributions to downstream Mn fluxes exceed continental runoff additions through all of the CAA channels and can be significant seasonally (Figure 6). The greater importance of glacial runoff for Mn results from reduced removal due to shorter travel distances and arrival times (Figure 8a), less dilution with many forms of outflow or smaller contributions from other external Mn sources, and larger characteristic Mn concentrations in glacial runoff in our model forcing. Based on our time series, glacial runoff constituent changes contribute about 3%–6% to net Mn fluxes across the important boundaries of Parry Channel, Nares Strait, and Baffin Bay annually. However, seasonal fluxes downstream can account for up to 18% of Mn transported across the Nares Strait boundary and up to 8% across Baffin Bay, representing a significant source of Mn (Figures 6a and 6b). Mn from continental runoff remains more contained within the southern channels of the CAA, while strong outflow from Nares Strait funnels Mn from glacial runoff directly downstream to Baffin Bay (Figure 3). This difference also suggests that the routing of runoff in this context controls the influence of the runoff on Mn in regions downstream.

Future projections indicate that increased phytoplankton nutrient limitation in Baffin Bay will lead to a decline in primary productivity (Kwiatkowski et al., 2019). While glacial runoff is high in macro- and micro-nutrients such as Mn and Fe (Bhatia et al., 2013, 2021), Hopwood et al. (2015) suggest that the physical circulation around Greenland hinders the export of Fe from the coast to the interior basin. In contrast to Fe, which has faster oxidation, for Mn, we saw indirect routing of glacial runoff contributions via Nares Strait and recirculation from Parry Channel which could contribute to Mn fluxes into Baffin Bay, highlighting the role of the CAA as a source of micronutrients downstream (Colombo et al., 2021).

4.4. Limitations of Results

The magnitude and spatial distribution of terrestrial runoff in the ocean is affected by confounding environmental changes such as enhanced discharge, the representation of runoff and sea ice in the physical model, model resolution, and for Mn: the treatment of scavenging, sinking, and removal of oxidized Mn, estuarine cycling, and characteristic Mn concentrations in runoff in the Mn model. We identify and explain the impact of these factors on the results below.

In this study, we focused on the oceanic impacts of biogeochemical constituent changes in terrestrial runoff, however discharge changes are another aspect of future predictions of the impact of runoff on biogeochemical constituents in the ocean (Feng et al., 2021; McClelland et al., 2006; Peterson et al., 2002) and are certainly an

important avenue for further research. Predicted increases in river discharge are associated with stronger stratification, suppression of mixing, and altered ocean dynamics. These factors are likely to increase the magnitude of runoff contributions to Mn in the surface ocean and potentially the extent of runoff influence. However, in Section 4.1, we identified that the runoff influence on Mn concentrations can extend beyond prevailing current directions in regions associated with strong mixing, suggesting that the suppression of mixing through stronger stratification could reduce the glacial runoff influence to Penny Strait and certain similar areas.

The spatial distribution of runoff in winter is impacted by sea ice (Section 4.1) and in this context, the model representation of sea ice. The model does not include land-fast ice and tides, resulting in more mobile ice than is generally observed. Specifically in the Beaufort Shelf region, the model does not represent the influence of land-fast ice build up which may result in farther offshore terrestrial freshwater transport in winter than in reality. In observations, offshore transport of freshwater is suppressed by the incorporation of freshwater into landfast ice and the spread of freshwater offshore is limited by the dam-like stamukhi in late winter (Macdonald et al., 1995). In addition, runoff in the model does not alter ocean heat content, so sea ice near river mouths may be overestimated in the model, suppressing offshore spread of this freshwater.

The terrestrial runoff forcing in the physical model does not vary interannually after 2010 and is limited by the number of available stream gauges in the Canadian Arctic (Bamber et al., 2012; Dai et al., 2009). As a result, we may underestimate the runoff contributions to the CAA and downstream Mn fluxes from 2010 to 2020. However, the dominant circulation patterns and ocean pathways are driven by the Arctic Ocean to North Atlantic pressure gradients and are thus relatively robust against these differences. Coupling of ocean models with runoff forcing derived from hydrological modeling of river catchment basins could improve these estimates. Hydrological model products also may have stronger continental runoff in the CAA than the Dai et al. (2009) dataset. Lastly, while the 1/12° resolution of this configuration allows the representation of freshwater fluxes associated with coastal currents, it is too coarse to represent physical processes associated with the land-ocean interface related to runoff, such as estuarine flow and sub-glacial melt plumes (Bhatia et al., 2021). In our model setup, we also do not distinguish between runoff from glaciers that extend into the marine system, or those that terminate on land and are drained by rivers. The dynamics of these runoff pathways differ in the amount of mixing present at the ocean interface which could impact the depth to which the Mn input extends. Nevertheless, when compared with hydrographic and remotely sensed observations (Section 4.1), the model represents the overall runoff flow in the ocean on the extensive spatial scale of this study.

Besides the physical factors described above, our estimates of the role of runoff on the ocean are a function of the treatment in the Mn model of: runoff magnitude and characteristic Mn content, estuarine cycling, scavenging and removal through sinking. The concentrations of riverine trace metals are relatively poorly constrained at peak discharge for smaller Arctic rivers. The resulting oceanic Mn influence pattern is unlikely to change, but the magnitude of additions can be greater as highlighted by our “seasonality” experiment. In this study, we chose not to incorporate the estuarine cycling of Mn and instead add only the dissolved fraction in discharge as larger portions of the dissolved fraction typically make it through the river-sea mixing zone (Gordeev et al., 2022). Heterogeneity in the chemical cycling within estuaries across our study domain could introduce finer scale variations in the contribution of Mn from runoff within our runoff type classification, and associated changes to the finer scale patterns of spatial extent. As discussed in Section 4.3, the flux of biogeochemical constituents downstream is also highly dependent on the removal rates, highlighting the need to constrain scavenging and sinking rates, and the factors that they depend on.

While our estimate of the magnitude of influence of Mn from terrestrial runoff should be taken as a first order estimate, the key results of the spatial extent and relative role of continental and glacial runoff are robust to the uncertainties described above.

5. Conclusion

Terrestrial runoff is an important source of geochemical constituents to the Arctic Ocean. The concentrations of (micro)nutrients in runoff are predicted to increase markedly with permafrost degradation, a transition from a surface water to a groundwater dominated system, and glacial melt (Bhatia et al., 2013; Spencer et al., 2015; Walvoord & Striegl, 2007). However, the extent to which changes to the terrestrial runoff impacts the marine environment is challenging to quantify. In this study, we conducted four experiments with a model for dissolved

manganese (Mn; Rogalla et al., 2022) in Inuit Nunangat or the CAA from 2002 to 2020 to identify the extent and magnitude of impact of glacial and continental runoff changes on Mn in the ocean and the role of runoff changes on downstream fluxes of micronutrients. We found that:

1. The heterogeneity in geochemical composition of Arctic runoff types creates distinct patterns of impact on the ocean in the CAA. As illustrated by dissolved Mn, the spatial extent of continental and glacial runoff contributions vary seasonally with changes in flow patterns, sea ice, and surface winds and the magnitude of the runoff contribution on Mn concentrations is primarily controlled by the characteristic Mn concentration in runoff during the freshet. While recent observations of trace elements in small rivers in the CAA provided a starting point for the terrestrial runoff contribution estimates in this study (Brown, Williams, et al., 2020; Colombo et al., 2019), further measurements of trace element concentrations at peak discharge in small rivers and better constrained estuarine removal rates for dissolved and particulate materials would significantly improve the estimates of the magnitude of runoff contributions on the biogeochemical composition of the ocean.
2. Terrestrial freshwater feeds micronutrients to two well-known polynyas in our domain: the Pikiyasorsuaq or North Water polynya (PNOW) and the Cape Bathurst polynya (Figures 3 and 7). Glacial runoff is rich in macro- and micro-nutrients such as Mn (Bhatia et al., 2013, 2021) and its presence in polynyas could help support high productivity rates. In our experiments, dissolved Mn from glacial runoff extends into the PNOW during late summer months when nutrients typically become limiting and may help support the long phytoplankton bloom durations and large bloom magnitudes observed in Kane Basin, Smith Sound, and the PNOW region (Marchese et al., 2017).
3. Glacial runoff dominates continental runoff changes to downstream dissolved Mn fluxes through the main channels of the CAA and may alter the biogeochemical composition of regions downstream. Local changes in glacial runoff contribute around 6% annually to Mn fluxes out of Nares Strait, and up to 18% seasonally. This seasonal peak is associated with the freshet and takes several days to months to reach the Nares Strait, Parry Channel, and Baffin Bay boundaries (Figure 8). These transit times could help estimate reductions to downstream transport of biogeochemical runoff constituents associated with scavenging and removal from the water column. Further studies to constrain removal rates and quantitative estimates of the factors controlling removal will help improve downstream Mn and other micronutrient flux estimates.

Data Availability Statement

The Mn model configuration, results, and analysis code are archived on FRDR at <https://doi.org/10.20383/103.0599> (Rogalla, 2023) and the Mn model code is available at <https://doi.org/10.20383/102.0388> (Rogalla, 2022). Analysis code is also available on Github at <https://github.com/brogalla/Mn-CAA-terrestrial-runoff>. Dissolved and particulate Mn observations in the Canadian Arctic Archipelago are available as part of the GEOTRACES Intermediate Data Product Group (2021) via the British Oceanographic Data Centre: <https://www.bodc.ac.uk/geotraces/data/idp2021/>. The numerical ocean model, NEMO, is available at <https://www.nemo-ocean.eu/> (Madec, 2008). For more details on the Arctic and Northern Hemispheric Atlantic 1/12° configuration (ANHA12) of NEMO, visit <http://knossos.eas.ualberta.ca/anha/anhatable.php>. All analysis was performed using Python 3 (Van Rossum & Drake, 2009) within Jupyter Notebooks with the NumPy, Pandas, Matplotlib, Seaborn, and cmocean packages (Harris et al., 2020; Hunter, 2007; Kluyver et al., 2016; The Pandas Development Team, 2020; Thyng et al., 2016; Waskom & the Seaborn development team, 2020).

References

- Ahmed, R., Prowse, T. D., Dibike, Y., Bonsal, B., & O'Neil, H. (2020). Recent trends in freshwater influx to the Arctic Ocean from four major Arctic-draining rivers. *Water*, 12(4), 1189. <https://doi.org/10.3390/w12041189>
- Aiken, G. R., Spencer, R. G. M., Striegl, R. G., Schuster, P. F., & Raymond, P. A. (2014). Influences of glacier melt and permafrost thaw on the age of dissolved organic carbon in the Yukon River basin. *Global Biogeochemical Cycles*, 28(5), 525–537. <https://doi.org/10.1002/2013gb004764>
- Alkire, M. B., Jacobson, A. D., Lehn, G. O., Macdonald, R. W., & Rossi, M. W. (2017). On the geochemical heterogeneity of rivers draining into the straits and channels of the Canadian Arctic Archipelago. *Journal of Geophysical Research: Biogeosciences*, 122(10), 2527–2547. <https://doi.org/10.1002/2016jg003723>
- Arfeuille, G. (2001). *On the freshwater transport through the southwest Canadian Arctic Archipelago due to buoyancy and wind forcing*. Doctoral dissertation, University of Victoria. <https://doi.org/10.1828/8792>
- Bacon, S., Marshall, A., Holliday, N. P., Aksenov, Y., & Dye, S. R. (2014). Seasonal variability of the east Greenland coastal current. *Journal of Geophysical Research: Oceans*, 119(6), 3967–3987. <https://doi.org/10.1002/2013jc009279>

Acknowledgments

We'd like to thank the anonymous reviewers for their helpful comments. The experiments in this study were conducted using computer resources provided by Compute Canada (RRG 2648 RAC 2019; RRG 2969 RAC 2020; RRG 1541 RAC 2021; RRG 1792 RAC 2022). The National Sciences and Engineering Council (NSERC) funded this work through the Climate Change and Atmospheric Research Grant: GEOTRACES (RGPC 433848-12) and an NSERC Discovery Grant (RGPIN-2016-03,865) to SEA. The University of British Columbia funded BR through a 4 year fellowship. The analysis scripts can be found on Github at <https://github.com/brogalla/Mn-CAA-terrestrial-runoff>, and the model setup and results can be downloaded from FRDR at <https://doi.org/10.20383/103.0599>.

- Bagard, M.-L., Chabaux, F., Pokrovsky, O. S., Viers, J., Prokushkin, A. S., Stille, P., et al. (2011). Seasonal variability of element fluxes in two central Siberian rivers draining high latitude permafrost dominated areas. *Geochimica et Cosmochimica Acta*, 75(12), 3335–3357. <https://doi.org/10.1016/j.gca.2011.03.024>
- Bamber, J., Van Den Broeke, M., Ettema, J., Lenaerts, J., & Rignot, E. (2012). Recent large increases in freshwater fluxes from Greenland into the North Atlantic. *Geophysical Research Letters*, 39(19). <https://doi.org/10.1029/2012gl052552>
- Bergeron, M., & Tremblay, J.-É. (2014). Shifts in biological productivity inferred from nutrient drawdown in the southern Beaufort Sea (2003–2011) and northern Baffin Bay (1997–2011), Canadian Arctic. *Geophysical Research Letters*, 41(11), 3979–3987. <https://doi.org/10.1002/2014gl059649>
- Bhatia, M. P., Kujawinski, E. B., Das, S. B., Breier, C. F., Henderson, P. B., & Charette, M. A. (2013). Greenland meltwater as a significant and potentially bioavailable source of iron to the ocean. *Nature Geoscience*, 6(4), 274–278. <https://doi.org/10.1038/ngeo1746>
- Bhatia, M. P., Waterman, S., Burgess, D. O., Williams, P. L., Bundy, R. M., Mellett, T., et al. (2021). Glaciers and nutrients in the Canadian Arctic Archipelago marine system. *Global Biogeochemical Cycles*, 35(8), e2021GB006976. <https://doi.org/10.1029/2021gb006976>
- Blais, M., Ardyna, M., Gosselin, M., Dumont, D., Bélanger, S., Tremblay, J.-É., et al. (2017). Contrasting interannual changes in phytoplankton productivity and community structure in the coastal Canadian Arctic Ocean. *Limnology & Oceanography*, 62(6), 2480–2497. <https://doi.org/10.1002/lno.10581>
- Bouillon, S., Morales Maqueda, M. A., Legat, V., & Fichefet, T. (2009). An elastic-viscous-plastic sea ice model formulated on Arakawa B and C grids. *Ocean Modelling*, 27(3–4), 174–184. <https://doi.org/10.1016/j.ocemod.2009.01.004>
- Bring, A., Fedorova, I., Dibike, Y., Hinzman, L., Mård, J., Mernild, S. H., et al. (2016). Arctic terrestrial hydrology: A synthesis of processes, regional effects, and research challenges. *Journal of Geophysical Research: Biogeosciences*, 121(3), 621–649. <https://doi.org/10.1002/2015jg003131>
- Brown, K. A., Holding, J. M., & Carmack, E. C. (2020). Understanding regional and seasonal variability is key to gaining a Pan-Arctic perspective on Arctic Ocean freshening. *Frontiers in Marine Science*, 7, 606. <https://doi.org/10.3389/fmars.2020.00606>
- Brown, K. A., Williams, W. J., Carmack, E. C., Fiske, G., François, R., McLennan, D., & Peucker-Ehrenbrink, B. (2020). Geochemistry of small Canadian Arctic rivers with diverse geological and hydrological settings. *Journal of Geophysical Research: Biogeosciences*, 125(1). <https://doi.org/10.1029/2019jg005414>
- Brunland, K. W., Orians, K. J., & Cowen, J. P. (1994). Reactive trace metals in the stratified central North Pacific. *Geochimica et Cosmochimica Acta*, 58(15), 3171–3182. [https://doi.org/10.1016/0016-7037\(94\)90044-2](https://doi.org/10.1016/0016-7037(94)90044-2)
- Carmack, E. C., Winsor, P., & Williams, W. J. (2015). The contiguous panarctic riverine coastal domain: A unifying concept. *Progress in Oceanography*, 139, 13–23. <https://doi.org/10.1016/j.pocean.2015.07.014>
- Carmack, E. C., Yamamoto-Kawai, M., Haine, T. W. N., Bacon, S., Bluhm, B. A., Lique, C., et al. (2016). Freshwater and its role in the Arctic Marine System: Sources, disposition, storage, export, and physical and biogeochemical consequences in the Arctic and global oceans. *Journal of Geophysical Research: Biogeosciences*, 121(3), 675–717. <https://doi.org/10.1002/2015jg003140>
- Chelton, D. B., Deszoeke, R. A., Schlax, M. G., Elmaggar, K., & Siwertz, N. (1998). Geographical variability of the first baroclinic Rossby Radius of deformation. *Journal of Physical Oceanography*, 28(3), 433–460. [https://doi.org/10.1175/1520-0485\(1998\)028<0433:gvotfb>2.0.co;2](https://doi.org/10.1175/1520-0485(1998)028<0433:gvotfb>2.0.co;2)
- Colombo, M., Brown, K. A., De Vera, J., Bergquist, B. A., & Orians, K. J. (2019). Trace metal geochemistry of remote rivers in the Canadian Arctic Archipelago. *Chemical Geology*, 525, 479–491. <https://doi.org/10.1016/j.chemgeo.2019.08.006>
- Colombo, M., Jackson, S. L., Cullen, J. T., & Orians, K. J. (2020). Dissolved iron and manganese in the Canadian Arctic Ocean: On the biogeochemical processes controlling their distributions. *Geochimica et Cosmochimica Acta*, 277, 150–174. <https://doi.org/10.1016/j.gca.2020.03.012>
- Colombo, M., Li, J., Rogalla, B., Allen, S. E., & Maldonado, M. T. (2022). Particulate trace element distributions along the Canadian Arctic GEOTRACES section: Shelf-water interactions, advective transport and contrasting biological production. *Geochimica et Cosmochimica Acta*, 323, 183–201. <https://doi.org/10.1016/j.gca.2022.02.013>
- Colombo, M., Rogalla, B., Li, J., Allen, S. E., Orians, K. J., & Maldonado, M. T. (2021). Canadian Arctic Archipelago shelf-ocean interactions: A major iron source to Pacific derived waters transiting to the Atlantic. *Global Biogeochemical Cycles*, 35(10), e2021GB007058. <https://doi.org/10.1029/2021gb007058>
- Dai, A., Qian, T., Trenberth, K. E., & Milliman, J. D. (2009). Changes in continental freshwater discharge from 1948 to 2004. *Journal of Climate*, 22(10), 2773–2792. <https://doi.org/10.1175/2008jcli2592.1>
- Feng, D., Gleason, C. J., Lin, P., Yang, X., Pan, M., & Ishitsuka, Y. (2021). Recent changes to Arctic river discharge. *Nature Communications*, 12(1), 1–9. <https://doi.org/10.1038/s41467-021-27228-1>
- Fichefet, T., & Maqueda, M. A. M. (1997). Sensitivity of a global sea ice model to the treatment of ice thermodynamics and dynamics. *Journal of Geophysical Research*, 102(C6), 12609–12646. <https://doi.org/10.1029/97jc00480>
- Fichot, C. G., Kaiser, K., Hooker, S. B., Amon, R. M. W., Babin, M., Bélanger, S., et al. (2013). Pan-Arctic distributions of continental runoff in the Arctic Ocean. *Scientific Reports*, 3(1), 1–6. <https://doi.org/10.1038/srep01053>
- Frey, K. E., & McClelland, J. W. (2009). Impacts of permafrost degradation on Arctic river biogeochemistry. *Hydrological Processes*, 23(1), 169–182. <https://doi.org/10.1002/hyp.7196>
- Gent, P. R., Willebrand, J., McDougall, T. J., & McWilliams, J. C. (1995). Parameterizing eddy-induced tracer transport in ocean circulation models. *Journal of Physical Oceanography*, 25(4), 463–474. [https://doi.org/10.1175/1520-0485\(1995\)025<0463:peitti>2.0.co;2](https://doi.org/10.1175/1520-0485(1995)025<0463:peitti>2.0.co;2)
- GEOTRACES Intermediate Data Product Group. (2021). *The GEOTRACES intermediate data product 2021 (IDP2021)* [Dataset]. NERC EDS British Oceanographic Data Centre NOC. <https://doi.org/10.5285/cf2d9ba9-d51d-3b7c-e053-8486abc0f5fd>
- Gillard, L. C., Hu, X., Myers, P. G., & Bamber, J. L. (2016). Meltwater pathways from marine terminating glaciers of the Greenland ice sheet. *Geophysical Research Letters*, 43(20), 10–873. <https://doi.org/10.1002/2016gl070969>
- Gordeev, V. V., Shevchenko, V. P., Novigatsky, A. N., Kochenkova, A. I., Starodymova, D. P., Lokhov, A. S., et al. (2022). The river–sea transition zone (marginal filter) of the northern Dvina river as an effective trap of riverine sedimentary matter on its way to the open area of the white sea. *Oceanology*, 62(2), 221–230. <https://doi.org/10.1134/s0001437022020060>
- Greene, C. H., & Pershing, A. J. (2007). Climate drives sea change. *Science*, 315(5815), 1084–1085. <https://doi.org/10.1126/science.1136495>
- Grenier, M., Brown, K. A., Colombo, M., Belhadji, M., Baconnais, I., Pham, V., et al. (2022). Controlling factors and impacts of river-borne neodymium isotope signatures and rare Earth element concentrations supplied to the Canadian Arctic Archipelago. *Earth and Planetary Science Letters*, 578, 117341. <https://doi.org/10.1016/j.epsl.2021.117341>
- Grivault, N., Hu, X., & Myers, P. G. (2018). Impact of the surface stress on the volume and freshwater transport through the Canadian Arctic Archipelago from a high-resolution numerical simulation. *Journal of Geophysical Research: Oceans*, 123(12), 9038–9060. <https://doi.org/10.1029/2018jc013984>
- Haine, T. W. N., Curry, B., Gerdes, R., Hansen, E., Karcher, M., Lee, C., et al. (2015). Arctic freshwater export: Status, mechanisms, and prospects. *Global and Planetary Change*, 125, 13–35. <https://doi.org/10.1016/j.gloplacha.2014.11.013>

- Hannah, C. G., Dupont, F., & Dunphy, M. (2008). Polynyas and tidal currents in the Canadian arctic archipelago. *Arctic*, 62(1), 83–95. <https://doi.org/10.14430/arctic115>
- Hansel, C. M. (2017). Manganese in marine microbiology. *Advances in Microbial Physiology*, 70, 37–83. <https://doi.org/10.1016/bs.ampbs.2017.01.005>
- Harris, C. R., Millman, K. J., van der Walt, S. J., Gommers, R., Virtanen, P., Cournapeau, D., et al. (2020). Array programming with NumPy [Software]. *Nature*, 585(7825), 357–362. <https://doi.org/10.1038/s41586-020-2649-2>
- Harwood, L. A., & Stirling, I. (1992). Distribution of ringed seals in the southeastern Beaufort Sea during late summer. *Canadian Journal of Zoology*, 70(5), 891–900. <https://doi.org/10.1139/z92-127>
- Hawkings, J. R., Skidmore, M. L., Wadham, J. L., Prisco, J. C., Morton, P. L., Hatton, J. E., et al. (2020). Enhanced trace element mobilization by Earth's ice sheets. *Proceedings of the National Academy of Sciences*, 117(50), 31648–31659. <https://doi.org/10.1073/pnas.2014378117>
- Heide-Jørgensen, M. P., Burt, L. M., Hansen, R. G., Nielsen, N. H., Rasmussen, M., Fossette, S., & Stern, H. (2013). The significance of the North Water polynya to Arctic top predators. *Ambio*, 42(5), 596–610. <https://doi.org/10.1007/s13280-012-0357-3>
- Hölemann, J. A., Schirmacher, M., & Prange, A. (2005). Seasonal variability of trace metals in the Lena River and the southeastern Laptev Sea: Impact of the spring freshet. *Global and Planetary Change*, 48(1–3), 112–125. <https://doi.org/10.1016/j.gloplacha.2004.12.008>
- Holmes, R. M., Coe, M. T., Fiske, G. J., Gurtovaya, T., McClelland, J. W., Shiklomanov, A. I., et al. (2013). Climate change impacts on the hydrology and biogeochemistry of arctic rivers. In C. R. Goldman, M. Kumagai, & R. D. Roberts (Eds.), *Climatic change and global warming of inland waters* (pp. 1–26). John Wiley and Sons, Ltd.
- Hopwood, M. J., Bacon, S., Arendt, K., Connelly, D. P., & Statham, P. J. (2015). Glacial meltwater from Greenland is not likely to be an important source of Fe to the North Atlantic. *Biogeochemistry*, 124(1–3), 1–11. <https://doi.org/10.1007/s10533-015-0091-6>
- Hu, X., Myers, P. G., & Lu, Y. (2019). Pacific water pathway in the Arctic Ocean and Beaufort Gyre in two simulations with different horizontal resolutions. *Journal of Geophysical Research: Oceans*, 124(8), 6414–6432. <https://doi.org/10.1029/2019JC015111>
- Hu, X., Sun, J., Chan, T. O., & Myers, P. G. (2018). Thermodynamic and dynamic ice thickness contributions in the Canadian Arctic Archipelago in NEMO-LIM2 numerical simulations. *The Cryosphere*, 12(4), 1233–1247. <https://doi.org/10.5194/tc-12-1233-2018>
- Hughes, K. G., Klymak, J. M., Hu, X., & Myers, P. G. (2017). Water mass modification and mixing rates in a 1/12 simulation of the Canadian Arctic Archipelago. *Journal of Geophysical Research: Oceans*, 122(2), 803–820. <https://doi.org/10.1002/2016JC012235>
- Hughes, K. G., Klymak, J. M., Williams, W. J., & Melling, H. (2018). Tidally modulated internal hydraulic flow and energetics in the central Canadian Arctic Archipelago. *Journal of Geophysical Research: Oceans*, 123(8), 5210–5229. <https://doi.org/10.1029/2018JC013770>
- Hunter, J. D. (2007). Matplotlib: A 2d graphics environment [software]. *Computing in Science & Engineering*, 9, 90–95. <https://doi.org/10.1109/mcse.2007.55>
- Ingram, R. G. (1981). Characteristics of the Great whale River plume. *Journal of Geophysical Research*, 86(C3), 2017–2023. <https://doi.org/10.1029/jc086ic03p02017>
- Jensen, L. T., Morton, P., Twining, B. S., Heller, M. I., Hatta, M., Measures, C. I., et al. (2020). A comparison of marine Fe and Mn cycling: US GEOTRACES GN01 Western Arctic case study. *Geochimica et Cosmochimica Acta*, 288, 138–160. <https://doi.org/10.1016/j.gca.2020.08.006>
- Jickells, T. D. (1999). The inputs of dust derived elements to the Sargasso Sea: A synthesis. *Marine Chemistry*, 68(1–2), 5–14. [https://doi.org/10.1016/s0304-4203\(99\)00061-4](https://doi.org/10.1016/s0304-4203(99)00061-4)
- Kadko, D., Aguilar-Islas, A., Bolt, C., Buck, C. S., Fitzsimmons, J. N., Jensen, L. T., et al. (2019). The residence times of trace elements determined in the surface Arctic Ocean during the 2015 US Arctic GEOTRACES expedition. *Marine Chemistry*, 208, 56–69. <https://doi.org/10.1016/j.marchem.2018.10.011>
- Kasper, J. L., & Weingartner, T. J. (2015). The spreading of a buoyant plume beneath a landfast ice cover. *Journal of Physical Oceanography*, 45(2), 478–494. <https://doi.org/10.1175/jpo-d-14-0101.1>
- Kluyver, T., Ragan-Kelley, B., Pérez, F., Granger, B., Bussonnier, M., & Frederic, J. (2016). *Jupyter Notebooks – A publishing format for reproducible computational workflows* [Software]. In F. Loizides, & B. Schmidt (Eds.). IOS Press. Retrieved from <https://jupyter.org/>
- Koch, J. C., Runkel, R. L., Striegl, R., & McKnight, D. M. (2013). Hydrologic controls on the transport and cycling of carbon and nitrogen in a boreal catchment underlain by continuous permafrost. *Journal of Geophysical Research: Biogeosciences*, 118(2), 698–712. <https://doi.org/10.1002/jgrg.20058>
- Kwiatkowski, L., Naar, J., Bopp, L., Aumont, O., Defrance, D., & Couespel, D. (2019). Decline in Atlantic primary production accelerated by Greenland Ice Sheet melt. *Geophysical Research Letters*, 46(20), 11347–11357. <https://doi.org/10.1029/2019gl085267>
- Lammers, R. B., Shiklomanov, A. I., Vörösmarty, C. J., Fekete, B. M., & Peterson, B. J. (2001). Assessment of contemporary Arctic river runoff based on observational discharge records. *Journal of Geophysical Research*, 106(D4), 3321–3334. <https://doi.org/10.1029/2000jd900444>
- Landing, W. M., & Bruland, K. W. (1980). Manganese in the North Pacific. *Earth and Planetary Science Letters*, 49(1), 45–56. [https://doi.org/10.1016/0012-821x\(80\)90149-1](https://doi.org/10.1016/0012-821x(80)90149-1)
- Landing, W. M., & Bruland, K. W. (1987). The contrasting biogeochemistry of iron and manganese in the Pacific Ocean. *Geochimica et Cosmochimica Acta*, 51(1), 29–43. [https://doi.org/10.1016/0016-7037\(87\)90004-4](https://doi.org/10.1016/0016-7037(87)90004-4)
- Lévy, M., Estublier, A., & Madec, G. (2001). Choice of an advection scheme for biogeochemical models. *Geophysical Research Letters*, 28(19), 3725–3728. <https://doi.org/10.1029/2001gl012947>
- Lique, C., Holland, M. M., Dibike, Y. B., Lawrence, D. M., & Screen, J. A. (2016). Modeling the Arctic freshwater system and its integration in the global system: Lessons learned and future challenges. *Journal of Geophysical Research: Biogeosciences*, 121(3), 540–566. <https://doi.org/10.1002/2015jg003120>
- Li Yung Lung, J. Y. S., Tank, S. E., Spence, C., Yang, D., Bonsal, B., McClelland, J. W., & Holmes, R. M. (2018). Seasonal and geographic variation in dissolved carbon biogeochemistry of rivers draining to the Canadian Arctic Ocean and Hudson Bay. *Journal of Geophysical Research: Biogeosciences*, 123(10), 3371–3386. <https://doi.org/10.1029/2018jg004659>
- Lovejoy, C., Legendre, L., Martineau, M. J., Bâcle, J., & Von Quillfeldt, C. H. (2002). Distribution of phytoplankton and other protists in the North Water. *Deep Sea Research Part II: Topical Studies in Oceanography*, 49(22–23), 5027–5047. [https://doi.org/10.1016/s0967-0645\(02\)00176-5](https://doi.org/10.1016/s0967-0645(02)00176-5)
- Macdonald, R. W., Paton, D. W., Carmack, E. C., & Omstedt, A. (1995). The freshwater budget and under-ice spreading of Mackenzie River water in the Canadian Beaufort Sea based on salinity and 18O/16O measurements in water and ice. *Journal of Geophysical Research*, 100(C1), 895–919. <https://doi.org/10.1029/94jc02700>
- Madec, G. (2008). NEMO ocean engine. *Note du Pôle de modélisation*, 27, 1288–1619. Institut Pierre-Simon Laplace. Retrieved from https://www.nemo-ocean.eu/wp-content/uploads/NEMO_book.pdf
- Marchese, C., Albouy, C., Tremblay, J.-É., Dumont, D., D'Ortenzio, F., Vissault, S., & Bélanger, S. (2017). Changes in phytoplankton bloom phenology over the North water (NOW) polynya: A response to changing environmental conditions. *Polar Biology*, 40(9), 1721–1737. <https://doi.org/10.1007/s00300-017-2095-2>

- Masina, S., Storto, A., Ferry, N., Valdivieso, M., Haines, K., Balmaseda, M., et al. (2017). An ensemble of eddy-permitting global ocean reanalyses from the MyOcean project. *Climate Dynamics*, 49(3), 813–841. <https://doi.org/10.1007/s00382-015-2728-5>
- McClelland, J. W., Déry, S. J., Peterson, B. J., Holmes, R. M., & Wood, E. F. (2006). A pan-arctic evaluation of changes in river discharge during the latter half of the 20th century. *Geophysical Research Letters*, 33(6), L06715. <https://doi.org/10.1029/2006gl025753>
- McClelland, J. W., Holmes, R. M., Dunton, K. H., & Macdonald, R. W. (2012). The Arctic Ocean estuary. *Estuaries and Coasts*, 35(2), 353–368. <https://doi.org/10.1007/s12237-010-9357-3>
- McClelland, J. W., Holmes, R. M., Peterson, B. J., Amon, R., Brabets, T., Cooper, L., et al. (2008). Development of a pan-Arctic database for river chemistry. *Eos, Transactions American Geophysical Union*, 89(24), 217–218. <https://doi.org/10.1029/2008eo240001>
- McClelland, J. W., Tank, S. E., Spencer, R. G. M., & Shiklomanov, A. I. (2015). Coordination and sustainability of river observing activities in the Arctic. *Arctic*, 68(5), 59–68. <https://doi.org/10.14430/arctic4448>
- McLaughlin, F., Carmack, E. C., Ingram, R., Williams, W. J., & Michel, C. (2004). In A. R. Robinson & K. H. Brink (Eds.), *Oceanography of the northwest passage, The Sea* (Vol. 14). chap. 31.
- Mei, Z.-P., Legendre, L., Gratton, Y., Tremblay, J.-É., LeBlanc, B., Mundy, C. J., et al. (2002). Physical control of spring-summer phytoplankton dynamics in the North Water, April–July 1998. *Deep Sea Research Part II: Topical Studies in Oceanography*, 49(22–23), 4959–4982. [https://doi.org/10.1016/s0967-0645\(02\)00173-x](https://doi.org/10.1016/s0967-0645(02)00173-x)
- Middag, R., De Baar, H. J. W., Laan, P., & Klunder, M. B. (2011). Fluvial and hydrothermal input of manganese into the Arctic Ocean. *Geochimica et Cosmochimica Acta*, 75(9), 2393–2408. <https://doi.org/10.1016/j.gca.2011.02.011>
- Moore, S. E., George, J. C., Coyle, K. O., & Weingartner, T. J. (1995). Bowhead whales along the Chukotka coast in autumn. *Arctic*, 48(2), 155–160. <https://doi.org/10.14430/arctic1237>
- Mulligan, R. P., & Perrie, W. (2019). Circulation and structure of the Mackenzie River plume in the coastal Arctic Ocean. *Continental Shelf Research*, 177, 59–68. <https://doi.org/10.1016/j.csr.2019.03.006>
- Münchow, A., & Garvine, R. W. (1993). Dynamical properties of a buoyancy-driven coastal current. *Journal of Geophysical Research*, 98(C11), 20063–20077. <https://doi.org/10.1029/93jc02112>
- Natural Resources Canada. (2010). Atlas of Canada: Distribution of freshwater - glaciers and icefields, Vol. 6(661). Retrieved from <https://open.canada.ca/data/en/dataset/e5ea9140-8893-11e0-858a-6cf049291510>
- Nijssen, B., O'Donnell, G. M., Hamlet, A. F., & Lettenmaier, D. P. (2001). Hydrologic sensitivity of global rivers to climate change. *Climate Change*, 50(1/2), 143–175. <https://doi.org/10.1023/a:1010616428763>
- Paucot, H., & Wollast, R. (1997). Transport and transformation of trace metals in the Scheldt estuary. *Marine Chemistry*, 58(1–2), 229–244. [https://doi.org/10.1016/s0304-4203\(97\)00037-6](https://doi.org/10.1016/s0304-4203(97)00037-6)
- Peterson, B. J., Holmes, R. M., McClelland, J. W., Vörösmarty, C. J., Lammers, R. B., Shiklomanov, A. I., et al. (2002). Increasing river discharge to the Arctic Ocean. *Science*, 298(5601), 2171–2173. <https://doi.org/10.1126/science.1077445>
- Pickart, R. S., Moore, G. W. K., Torres, D. J., Fratantoni, P. S., Goldsmith, R. A., & Yang, J. (2009). Upwelling on the continental slope of the Alaskan Beaufort Sea: Storms, ice, and oceanographic response. *Journal of Geophysical Research*, 114(C1), C00A13. <https://doi.org/10.1029/2008jc005009>
- Pokrovsky, O. S., Viers, J., Shirokova, L. S., Shevchenko, V. P., Filipov, A. S., & Dupré, B. (2010). Dissolved, suspended, and colloidal fluxes of organic carbon, major and trace elements in the Severnaya Dvina River and its tributary. *Chemical Geology*, 273(1–2), 136–149. <https://doi.org/10.1016/j.chemgeo.2010.02.018>
- Prinsenbergh, S., Hamilton, J., Peterson, I., & Pettipas, R. (2009). Observing and interpreting the seasonal variability of the oceanographic fluxes passing through Lancaster Sound of the Canadian Arctic Archipelago. In J. C. J. Nihoul & A. G. Kostianoy (Eds.), *Influence of climate change on the changing Arctic and sub-Arctic conditions* (pp. 125–143). Springer Netherlands.
- Prowse, T. D., Bring, A., Mård, J., Carmack, E., Holland, M., Instanes, A., et al. (2015). Arctic freshwater synthesis: Summary of key emerging issues. *Journal of Geophysical Research: Biogeosciences*, 120(10), 1887–1893. <https://doi.org/10.1002/2015jg003128>
- Prowse, T. D., & Flegg, P. O. (2000). Arctic river flow: A review of contributing areas. In E. L. Lewis, E. P. Jones, P. Lemke, T. D. Prowse, & P. Wadhams (Eds.), *The freshwater budget of the Arctic Ocean* (Vol. 70, pp. 269–280). Springer Netherlands. https://doi.org/10.1007/978-94-011-4132-1_12
- Rogalla, B. (2022). Mn model of the Canadian Arctic Archipelago and the Canada Basin - Model output and code for Rogalla et al. 2022 [Dataset]. Federated Research Data Repository/dépôt fédéré de données de recherche. <https://doi.org/10.20383/102.0388>
- Rogalla, B. (2023). Mn model terrestrial runoff sensitivity experiments of the Canadian Arctic Archipelago ocean - Model output and setup for Rogalla et al. 2023 [Dataset]. Federated Research Data Repository/dépôt fédéré de données de recherche. <https://doi.org/10.20383/102.0388>
- Rogalla, B., Allen, S. E., Colombo, M., Myers, P. G., & Orians, K. J. (2022). Sediments in sea ice drive the Canada basin surface Mn maximum: Insights from an Arctic Mn ocean model. *Global Biogeochemical Cycles*, 36(8). <https://doi.org/10.1029/2022GB007320>
- Saunders, P. A., Deibel, D., Stevens, C. J., Rivkin, R. B., Lee, S. H., & Klein, B. (2003). Copepod herbivory rate in a large arctic polynya and its relationship to seasonal and spatial variation in copepod and phytoplankton biomass. *Marine Ecology Progress Series*, 261, 183–199. <https://doi.org/10.3354/meps261183>
- Serreze, M. C., Barrett, A. P., Slater, A. G., Woodgate, R. A., Aagaard, K., Lammers, R. B., et al. (2006). The large-scale freshwater cycle of the Arctic. *Journal of Geophysical Research*, 111(C11), C11010. <https://doi.org/10.1029/2005jc003424>
- Shen, Y., Benner, R., Robbins, L. L., & Wynn, J. G. (2016). Sources, distributions, and dynamics of dissolved organic matter in the Canada and Makarov basins. *Frontiers in Marine Science*, 3, 198. <https://doi.org/10.3389/fmars.2016.00198>
- Shiller, A. M. (1997). Manganese in surface waters of the Atlantic Ocean. *Geophysical Research Letters*, 24(12), 1495–1498. <https://doi.org/10.1029/97gl01456>
- Sim, N. (2018). *Biogeochemical cycling of dissolved and particulate manganese in the northeast Pacific and Canadian western Arctic*. Doctoral dissertation, University of British Columbia. <https://doi.org/10.14288/1.0374222>
- Simpson, J. H. (1997). Physical processes in the ROFI regime. *Journal of Marine Systems*, 12(1–4), 3–15. [https://doi.org/10.1016/s0924-7963\(96\)00085-1](https://doi.org/10.1016/s0924-7963(96)00085-1)
- Smith, G. C., Roy, F., Mann, P., Dupont, F., Brasnett, B., Lemieux, J.-F., et al. (2014). A new atmospheric dataset for forcing ice-ocean models: Evaluation of reforecasts using the Canadian global deterministic prediction system. *Quarterly Journal of the Royal Meteorological Society*, 140(680), 881–894. <https://doi.org/10.1002/qj.2194>
- Spencer, R. G. M., Mann, P. J., Dittmar, T., Eglinton, T. I., McIntyre, C., Holmes, R. M., et al. (2015). Detecting the signature of permafrost thaw in Arctic rivers. *Geophysical Research Letters*, 42(8), 2830–2835. <https://doi.org/10.1002/2015gl063498>
- Stadnyk, T. A., MacDonald, M. K., Tefs, A., Déry, S. J., Koenig, K., Gustafsson, D., et al. (2020). Hydrological modeling of freshwater discharge into Hudson Bay using HYPE. *Elementa: Science of the Anthropocene*, 8. <https://doi.org/10.1525/elementa.439>

- Stegall, S. T., & Zhang, J. (2012). Wind field climatology, changes, and extremes in the Chukchi-Beaufort seas and Alaska north slope during 1979-2009. *Journal of Climate*, 25(23), 8075–8089. <https://doi.org/10.1175/jcli-d-11-00532.1>
- Sunda, W. G. (2012). Feedback interactions between trace metal nutrients and phytoplankton in the ocean. *Frontiers in Microbiology*, 3, 204. <https://doi.org/10.3389/fmicb.2012.00204>
- Sunda, W. G., & Huntsman, S. A. (1994). Photoreduction of manganese oxides in seawater. *Marine Chemistry*, 46(1–2), 133–152. [https://doi.org/10.1016/0304-4203\(94\)90051-5](https://doi.org/10.1016/0304-4203(94)90051-5)
- Tank, S. E., Manizza, M., Holmes, R. M., McClelland, J. W., & Peterson, B. J. (2012). The processing and impact of dissolved riverine nitrogen in the Arctic Ocean. *Estuaries and Coasts*, 35(2), 401–415. <https://doi.org/10.1007/s12237-011-9417-3>
- Tao, R., & Myers, P. G. (2022). Modelling the oceanic advection of pollutants spilt along with the Northwest Passage. *Atmosphere-Ocean*, 60(2), 1–14. <https://doi.org/10.1080/07055900.2022.2065965>
- The Pandas Development Team. (2020). Pandas-dev/pandas: Pandas [Software]. *Zenodo*, 21, 1–9. <https://doi.org/10.5281/zenodo.3509134>
- Thyng, K. M., Greene, C. A., Hetland, R. D., Zimmerle, H. M., & DiMarco, S. F. (2016). True colors of oceanography: Guidelines for effective and accurate colormap selection [Software]. *Oceanography*, 29, 9–13. <https://doi.org/10.5670/oceanog.2016.66>
- Tremblay, J.-É., Gratton, Y., Carmack, E. C., Payne, C. D., & Price, N. M. (2002). Impact of the large-scale Arctic circulation and the North water polynya on nutrient inventories in Baffin Bay. *Journal of Geophysical Research*, 107(C8), 3112. <https://doi.org/10.1029/2000jc000595>
- Turner, A., Millward, G. E., & Morris, A. W. (1991). Particulate metals in five major North Sea estuaries. *Estuarine, Coastal and Shelf Science*, 32(4), 325–346. [https://doi.org/10.1016/0272-7714\(91\)90047-f](https://doi.org/10.1016/0272-7714(91)90047-f)
- Van Genuchten, C. M., Hopwood, M. J., Liu, T., Krause, J., Achterberg, E. P., Rosing, M. T., & Meire, L. (2022). Solid-phase Mn speciation in suspended particles along meltwater-influenced fjords of West Greenland. *Geochimica et Cosmochimica Acta*, 326, 180–198. <https://doi.org/10.1016/j.gca.2022.04.003>
- Van Hulten, M., Middag, R., Dutay, J.-C., De Baar, H., Roy-Barman, M., Gehlen, M., et al. (2017). Manganese in the west Atlantic Ocean in the context of the first global ocean circulation model of manganese. *Biogeosciences*, 14(5), 1123–1152. <https://doi.org/10.5194/bg-14-1123-2017>
- Vannote, R. L., Minshall, G. W., Cummins, K. W., Sedell, J. R., & Cushing, C. E. (1980). The river continuum concept. *Canadian Journal of Fisheries and Aquatic Sciences*, 37(1), 130–137. <https://doi.org/10.1139/f80-017>
- Van Rossum, G., & Drake, F. L. (2009). *Python 3 reference manual* [Software]. CreateSpace.
- Walvoord, M. A., & Striegl, R. G. (2007). Increased groundwater to stream discharge from permafrost thawing in the Yukon river basin: Potential impacts on lateral export of carbon and nitrogen. *Geophysical Research Letters*, 34(12), L12402. <https://doi.org/10.1029/2007gl030216>
- Wang, Q., Myers, P. G., Hu, X., & Bush, A. B. G. (2012). Flow constraints on pathways through the Canadian Arctic Archipelago. *Atmosphere-Ocean*, 50(3), 373–385. <https://doi.org/10.1080/07055900.2012.704348>
- Waskom, M., & The Seaborn development team. (2020). Seaborn [Software]. *Zenodo*. <https://doi.org/10.5281/zenodo.592845>
- White, D., Hinzman, L., Alessa, L., Cassano, J., Chambers, M., Falkner, K., et al. (2007). The Arctic freshwater system: Changes and impacts. *Journal of Geophysical Research*, 112(G4). <https://doi.org/10.1029/2006jg000353>
- Yamamoto-Kawai, M., Carmack, E. C., McLaughlin, F. A., & Falkner, K. K. (2010). Oxygen isotope ratio, barium and salinity in waters around the North American coast from the Pacific to the Atlantic: Implications for freshwater sources to the Arctic through flow. *Journal of Marine Research*, 68(1), 97–117. <https://doi.org/10.1357/002224010793078988>
- Yamamoto-Kawai, M., McLaughlin, F. A., Carmack, E. C., Nishino, S., Shimada, K., & Kurita, N. (2009). Surface freshening of the Canada Basin, 2003–2007: River runoff versus sea ice meltwater. *Journal of Geophysical Research*, 114(C1), C00A05. <https://doi.org/10.1029/2008jc005000>
- Zhou, J. L., Liu, Y. P., & Abrahams, P. W. (2003). Trace metal behaviour in the Conwy estuary, north Wales. *Chemosphere*, 51(5), 429–440. [https://doi.org/10.1016/s0045-6535\(02\)00853-6](https://doi.org/10.1016/s0045-6535(02)00853-6)